AD NUMBER

AD480948

LIMITATION CHANGES

TO:

Approved for public release; distribution is unlimited.

FROM:

**Distribution authorized to U.S. Gov't. agencies and their contractors;
Administrative/Operational Use; JAN 1966. Other requests shall be referred to Air Force Materials Lab., Wright-Patterson AFB, OH 45433.**

AUTHORITY

AFML ltr 22 Aug 1968

AFML-TR-65-2
Part I, Volume VI

TERNARY PHASE EQUILIBRIA IN TRANSITION METAL-BORON-CARBON-SILICON SYSTEMS

Part I. Related Binary Systems

Volume VI. W-C System: Supplemental Information on the Mo-C System

E. Rudy
St. Windisch
J. R. Hoffman

Aerojet-General Corporation

TECHNICAL REPORT NO. AFML-TR-65-2, Part I, Volume VI
January 1966

Air Force Materials Laboratory
Research and Technology Division
Air Force Systems Command
Wright-Patterson Air Force Base, Ohio

NOTICES

When Government drawings, specifications, or other data are used for any purpose other than in connection with a definitely related Government procurement operation, the United States Government thereby incurs no responsibility nor any obligation whatsoever; and the fact that the Government may have formulated, furnished, or in any way supplied the said drawings, specifications, or other data, is not to be regarded by implication or otherwise as in any manner licensing the holder or any other person or corporation, or conveying any rights or permission to manufacture, use or sell any patented invention that may in any way be related thereto.

Copies of this report should not be returned to the Research and Technology Division unless return is required by security considerations, contractual obligations, or notice on a specific document.

Form 1473

(6) TERNARY PHASE EQUILIBRIA IN TRANSITION METAL-BORON-CARBON-SILICON SYSTEMS.

Part I. Related Binary Systems.

Volume VI. W-C System: Supplemental Information on the Mo-C System.

(9) Technical rept.,

(10) E. Rudy,
St. Windisch and
J. R. Hoffman,

(11) Jan 66,

(12) 79p.

(15) AF 33 (615)-1249

(16) AF-7350

(17) 735001

(18) AFML

(19) TR-65-2-Pt-1-Vol-6

12

FOREWORD

The research described in this report was carried out at the Materials Research Laboratory, Aerojet-General Corporation, Sacramento, California, under USAF Contract No. AF 33(615)-1249. The contract was initiated under Project No. 7350, Task No. 735001, and was administered under the direction of the Air Force Materials Laboratory, Research and Technology Division, with Captain R. A. Peterson and Lt. P.J. Marchiando acting as Project Engineers, and Dr. E. Rudy, Aerojet-General Corporation, as Principal Investigator. Professor Dr. Hans Nowotny, University of Vienna, served as consultant to the program.

The project, which includes the experimental and theoretical investigation of related binary and ternary systems in the system classes Me_1-Me_2-C, Me-B-C, Me_1-Me_2-B, Me-Si-B, and Me-Si-C, was initiated on 1 January 1964. The work on related binary systems Me-C and Me-B was initiated November 1964 as a subtask to the investigation of the ternaries.

The experimental work on this system was performed by E. Rudy and St. Windisch. Assisting in the investigations were: H. D. Heetderks (DTA-runs), J. Pomodoro (sample preparation), J. Hoffman (Metallographic preparations), and R. Cobb (X-ray exposures). The chemical analytical work was carried out under the supervision of Mr. W. E. Trahan, Quality Control Division, Solid Rocket Operation.

The help of Mr. R. Cristoni in preparing the numerous drawings and of Mrs. J. Weidner, who typed the report, is gratefully acknowledged.

The manuscript of this report was released by the authors September 1965 for publication as an RTD Technical Report.

Other reports issued under USAF-Contract AF 33(615)-1249 have included:

Part I. Related Binaries
- Volume I. Mo-C System
- Volume II. Ti-C and Zr-C System
- Volume III. Mo-B and W-B Systems
- Volume IV. Hf-C System
- Volume V. Ta-C System

Part II. Ternary Systems
- Volume I. Ta-Hf-C System
- Volume II. Ti-Ta-C System
- Volume III. Zr-Ta-C System
- Volume IV. Zr-Hf-C, Ti-Hf-C and Ti-Zr-C Systems

Part III. Special Experimental Techniques
Volume I. High Temperature Differential Thermal Analysis

Part IV. Thermochemical Calculations
Volume I. Thermodynamic Properties of Group IV, V, and VI Binary Transition Metal Carbides

This technical report has been reviewed and is approved.

W. G. RAMKE
Chief, Ceramics and Graphite Branch
Materials and Ceramics Division
Air Force Materials Laboratory

ABSTRACT

The alloy system tungsten-carbon was investigated by means of X-ray, DTA, and melting point techniques on chemically analyzed alloys, and a complete phase diagram was established.

Supplementary investigations performed on the molybdenum-carbon system are in confirmation of our previous findings regarding the α-β-Mo_2C phase separation as well as the phase relations between η- and α-MoC_{1-x}.

The results are discussed and compared with previously reported system data, Part I, Volume I.

TABLE OF CONTENTS

TABLE OF CONTENTS (Cont.)

ILLUSTRATIONS

ILLUSTRATIONS (Cont.)

ILLUSTRATIONS (Cont.)

ILLUSTRATIONS (Cont.)

ILLUSTRATIONS (Cont.)

TABLES

I. INTRODUCTION AND SUMMARY

A. INTRODUCTION

A continuation of our efforts on the elucidation of the high temperature phase relationships in binary and ternary systems of refractory transition metals with carbon, boron, and silicon, a complete investigation of the system tungsten-carbon has been undertaken, and a phase diagram was established. Supplementary investigations were undertaken on the Mo-C system in order to confirm the existence of α- and β-Mo_2C, and of η-MoC_{1-x} and σ-MoC_{1-x} as four distinct phases in the high temperature (>2200°C) region. The finally adopted phase diagrams deviate only in minor details from the results presented in previous reports[1, 2, 3].

For the investigations in the tungsten-carbon system, an excellent reference was available from the recent work by R. T. Dolloff and R. V. Sara[4, 5]. Areas of concern were the high temperature carbon-rich homogeneity range of the cubic phase, and the type of decomposition of WC at high temperatures. Since a high temperature polymorph of W_2C has been reported in earlier work[6-9] and phase transitions of the Me_2C-phases had been found by us in other carbide systems[3, 10, 11], a contest of the earlier work seemed to be advisable. Further data of interest and of importance for the establishment of the high-carbon portions in tungsten-containing ternary metal-carbon systems, performed under this program, concerned the composition of the liquidus line of the equilibrium melt-graphites; a fairly comprehensive study of the carbon-rich portion of the system tungsten-carbon was therefore included in the overall experimental task.

B. SUMMARY

1. Tungsten-Carbon

Four intermetallic phases [α-W_2C, β-W_2C, α-WC_{1-x} (B1), and WC] from which only one (WC) is stable at temperatures below 1250°C, occur in the system. The system details are as follows:

a. Tungsten

The melting point of tungsten, determined on cold-pressed and high-vacuum sintered specimens, was found to be 3423 $\pm$ 10°C (mean of three determinations). The terminal solid solubility of carbon in tungsten was not specifically investigated, but found to be less than 0.5 At% at 2710°C, the temperature of the W + W_2C eutectic.

b. α-Ditungsten-Carbide (α-W_2C)

α-W_2C, with a hexagonal close-packed arrangement of metal atoms, extends from 29.2 At% C (a = 2.985 Å, c = 4.717 Å) to the stoichiometric composition (a = 3.001 Å, c = 4.728 Å) at 2200°C, and from 25.6 to 32 At% C at the eutectic temperature W-W_2C (2710°C). The phase melts congruently at 2776 $\pm$ 7°C at a composition of 31 At% C. Below approximately 1250°C, α-W_2C decomposes in an extremely slow eutectoid reaction into WC and W and forms a eutectic with tungsten; the eutectic point is located at 22 At% C and 2710°C.

c. β-Ditungsten-Carbide (β-W_2C)

The β-W_2C phase, which is unstable below approximately 2450°C, decomposes peritectically at ~2750°C into α-W_2C and melt. The boundaries of the phase are confined to the compositional

limits of 32 to 35 At% C. The appearance of this phase may be regarded as being the result of a phase-separation of W_2C due to a disordering reaction occurring in the carbon sublattice, with the structure of the tungsten host-lattice not being affected by the transformation process. The α-β-W_2C phase reaction may be interpreted such, that at substoichiometric compositions, the disordering proceeds as a homogeneous (single phased) reaction, while hyperstoichiometric compositions undergo a discontinuous phase change.

The high temperature (less ordered) phase could not be completely retained by quenching. The cell dimensions, obtained from tin-quenched alloys, were: a = 3.002 Å, c = 4.75-4.76 Å.

d. The Cubic High Temperature Phase (α-WC_{1-x})

In view of its isomorphy with α-MoC_{1-x}, this high temperature phase was designated as α-WC_{1-x}. It has a face-centered cubic (B1-type) of structure, with a = 4.220 $\pm$ 1 Å, and decomposes in a rapid eutectoid reaction at 2530 $\pm$ 20°C into β-W_2C and WC. Its homogeneity limits are confined to compositions between 37.5 to 40 At% C. α-WC_{1-x} melts congruently at 2747 $\pm$ 8°C at a composition of 39 At% C, and forms eutectic equilibria with β-W_2C (36.5 At% C, 2735 $\pm$ 6°C), and WC (41 At% C, 2720 $\pm$ 10°C).

e. Tungsten Monocarbide (WC)

Tungsten monocarbide, with a negligible range of homogeneity over the entire temperature range of existence, has a simple hexagonal unit cell with a = 2.906 Å, c = 2.837 Å; it decomposes in a peritectic reaction at 2776 $\pm$ 4°C (42 At% C) into melt and graphite.

The liquidus line of the equilibrium $(W,C)_{(\ell)}$—$C_{(gr.)}$ was determined to 3800°C. The carbon content of the graphite-saturated melt increases nearly linearly from 42 At% C at the WC peritectic temperature (2776°C), to 60 At% C at the sublimation temperature of graphite (3800 ± 50°C).

The experimental findings are summarized in the phase diagram shown in Figure 1. The isothermal reactions are listed in Table 1.

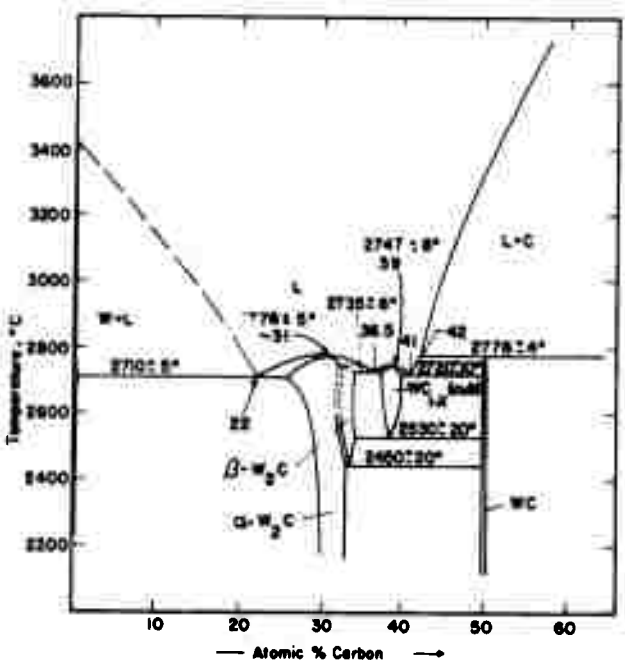

Figure 1. The Phase Diagram of the System Tungsten-Carbon

[The temperature figures given refer to the precision of the measurements and do not include the pyrometer calibration errors. Sect. III-2]

Table 1. Isothermal Reactions in the Tungsten-Carbon System

Temperature °C	Reaction	Composition of the Equilibrium Phases At% C			Type of Reaction
2776	$L \rightarrow \alpha\text{-}W_2C$	31	31	-	Congruent Transformation
2776	$L + C \rightarrow WC$	42	~100	50	Peritectic Reaction
~2750	$L + \alpha\text{-}W_2C \rightarrow \beta\text{-}W_2C$	~35	~32	~33	Peritectic Reaction
2735	$L \rightarrow \beta\text{-}W_2C + \alpha\text{-}WC_{1-x}$	36.5	~34	~37	Eutectic Reaction
2720	$L \rightarrow \alpha\text{-}WC_{1-x} + WC$	41	39	~50	Eutectic Reaction
2710	$L \rightarrow W + \alpha\text{-}W_2C$	22	< 0.1	25.6	Eutectic Reaction
2530	$\alpha\text{-}WC_{1-x} \rightarrow \beta\text{-}W_2C + WC$	37.5	~34.5	~50	Eutectoid Reaction
2450	$\beta\text{-}W_2C \rightarrow \alpha\text{-}W_2C + WC$	~34	~33	~50	Eutectoid Reaction
1250	$\alpha\text{-}W_2C \rightarrow W + WC$	≈32	~0	~50	Eutectoid Reaction

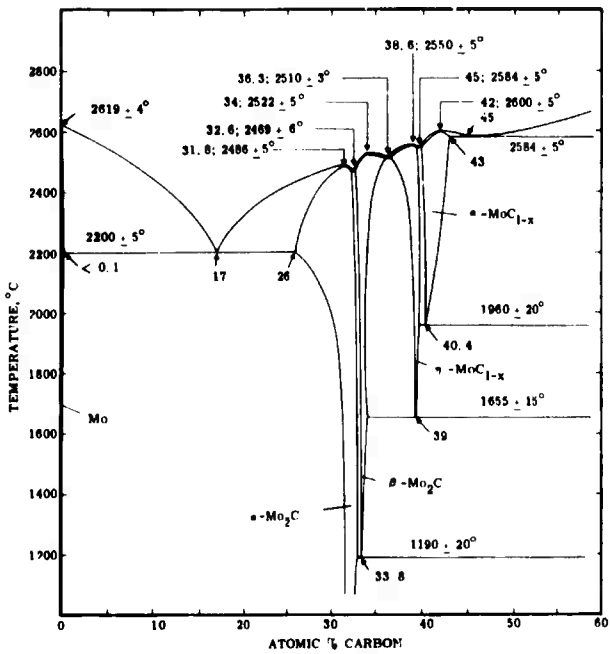

Figure 2. Phase Diagram of the System Molybdenum-Carbon

2. Molybdenum-Carbon

Diffusion-couple experiments performed on Mo-C alloys substantiated and confirmed our previous findings, namely, that α-Mo_2C, β-Mo_2C, η-MoC_{1-x}, α-MoC_{1-x} exist as discrete phases at high temperatures.

DTA-investigations carried out on closely spaced samples in the concentration region from 29 to 35 atomic percent carbon showed a steep dependence of the onset of the disordering reaction on the composition; while in samples with 33 At% C an average reaction temperature of 1450°C was measured[3], the eutectoid decomposition of the β-phase at somewhat higher carbon concentrations (33.5 to 33.8 At% C)

was found to converge at a temperature of 1190 ± 20°C. The width of the concentration gap between α- and β-Mo_2C, as well as η-MoC_{1-x} and α-MoC_{1-x} is difficult to assess experimentally, but is probably much less than 1 atomic % carbon. The resulting phase diagram, refined by the newly gained information is shown in Figure 2.

II. LITERATURE REVIEW

The currently accepted tungsten-carbon phase diagram, based mainly on the work by R. T. Doloff and R. V. Sara[4, 5] is shown in Figure 3. A complete previous investigation of the system was carried out by W. P. Sykes[12] (Figure 4).

The existence of at least three intermetallic phases W_2C, α-WC_{1-x} and WC, has been established from previous investigations and their structures have been clarified.

W_2C has a hexagonal close-packed arrangement of metal atoms[13], with a = 2.992, and c = 4.722 Å. According to L.N. Butorina and Z.G. Pinsker[16], who studied this compound by electron diffraction techniques, W_2C has the anti-cadmium-iodide (C 6) type of structure (ordered distribution of carbon atoms) and not the L'3 type (statistical distribution of the carbon atoms among the 0 and 1/2 layer), as assumed previously[17, 25, 27].

A summary of recent lattice parameter determinations is presented in Table 2[17]. According to R. T. Doloff and R. V. Sara[4, 5], the phase extends from 28 to 33.3 At% C at 2460°C. The homogeneity range decreases towards lower temperatures, extending from ~31 to 33 At% at 1400°C[18, 19].

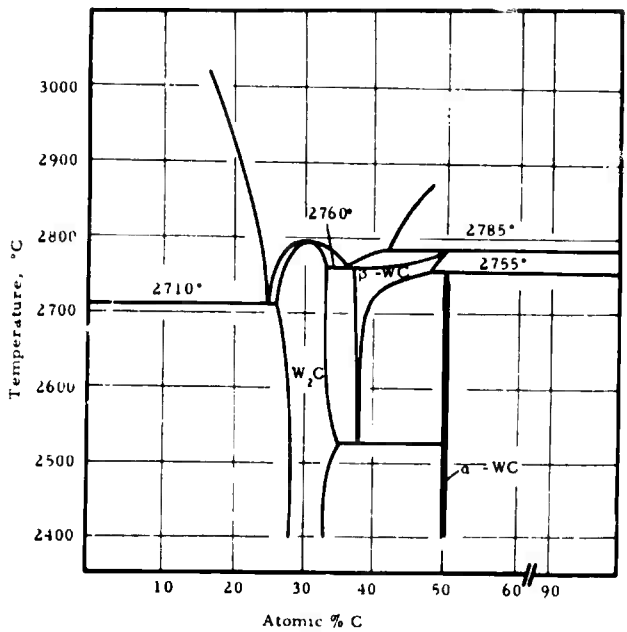

Figure 3. Tungsten-Carbon Phase Diagram.
(R. T. Doloff and R. V. Sara, 1962)

Across the homogeneous range, the c-spacing increases with increasing carbon content, whereas the a-axis remains practically constant[19]. According to G. W. Orton[20], W_2C is unstable below approximately 1250°C, decomposing into tungsten and the monocarbide.

There seems to be some uncertainty regarding a polymorphic phase change of W_2C at high temperatures: In gas-phase carburized tungsten wires, F. Skaupy[6] and K. Becker[7, 8, 9] observed the formation of a new phase β-W_2C, which is unstable below 2400°C. Although the structure could not be clarified, the X-ray patterns showed a close structural

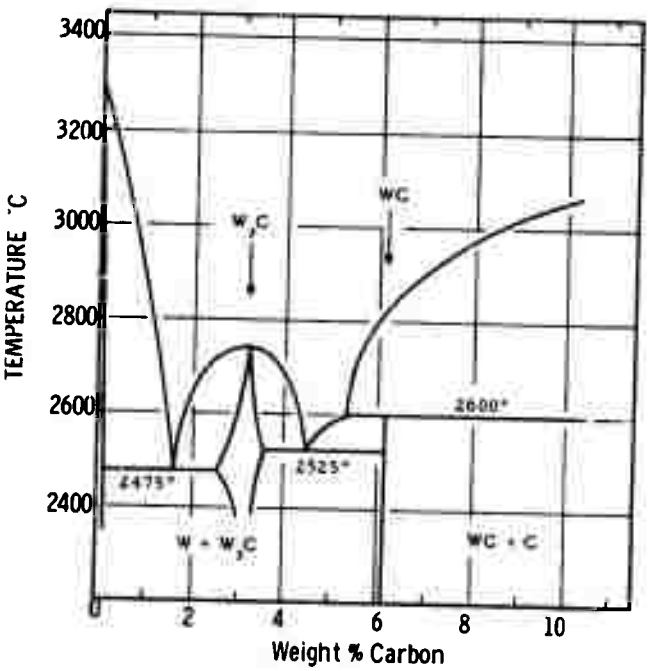

Figure 4. Tungsten-Carbon Phase Diagram.
(R. Kieffer and F. Benesovsky, After Data by W. P. Sykes, 1930)

similarity to the low temperature modification of W_2C. The modification change of W_2C was not observed by W. P. Sykes[12], and also was not confirmed in the exhaustive recent system work by R.T. Doloff and R. V. Sara[4].

In flame-sprayed tungsten carbide layers, K.Kirner[21] observed the formation of a cubic (B1) 'WC' with a cell dimension of ~4.23 Å. Apparently the same compound, but designated as β-W_2C, had been observed by G. Lautz and D. Schneider[22], and by H. J. Goldschmidt

Table 2. Structure and Lattice Parameters of Tungsten Carbides

Phase	Structure	Lattice Parameters, Å	
		Literature Values	This Investigation (Quenched Alloys)
W_2C	hex.[13] C6-type[16]	a = 2.992, c = 4.721 (37); a = 2.993, c = 4.727 (38) a = 2.992, c = 4.722 (13) a = 2.99, c = 4.69 } W_2C + W a = 2.99, c = 4.82 } W_2C + W	a = 2.985, c = 4.717 at 29.2 At% C a = 3.001, c = 4.728 at 33.3 At% C
α-WC_{1-x} (β-WC[4,5])	Cub., B1	a = 4.23 (21) a = 4.16 ('β-W_2C'?) (39) a = 4.25 ('β-W_2C') (23) a = 4.215 (45 At% C) (4, 5)	a = 4.220 ± 1 Å (~38 At% C)
WC	hexag.	a = 2.907, c = 2.837 (40); a = 2.906-7, c = 2.837-9 (38) a = 2.9063, c = 2.8368 (41); a = 2.900, c = 2.831 (13)	a = 2.906, c = 2.837 ($WC_{1.0}$)

and J. A. Brand[23] as products of arc-discharges between WC-electrodes, or between electrodes of tungsten and graphite. DTA- and metallographic experiments performed by R. T. Doloff and R. V. Sara[4, 5] showed, that the cubic phase is unstable below 2525°C, decomposing into W_2C and WC. The eutectoid composition lies at 37.5 At.% C; above 2700°C the phase extends to the ideal composition WC[4, 5].

Tungsten monocarbide has a hexagonal unit cell, with a = 2.906 Å, c = 2.837 Å (Table 1). The structure consists of two interpenetrating simple hexagonal lattices[13, 14, 24, 25] (ordered distribution of carbon atoms) thus ruling out the B_8-type (partially disordered NiAs-type), proposed as an alternative possibility by G. Hägg[26]. The homogeneity range of tungsten monocarbide is probably below 1 atomic percent[17, 25].

Systematic studies of the phase relations in the system have been performed by O. Ruff and R. Wunsch[28], A. Westgren and G. Phragmen[13], K. Becker and R. Holbling[29], F. Skaupy[6], J.L. Gregg and C.W. Küttner[30], S. L. Hoyt[31], and particularly by P. W. Sykes[12] (Figure 4). More recent investigations by R. T. Doloff and R. V. Sara[4] showed, that the high temperature phase relationships in the system are more complicated than previously anticipated (Figure 3). According to the latter authors, W_2C melts congruently, while the monocarbide (B1) decomposes peritectically at temperatures close to 2800°C (Table 3).

The W-W_2C eutectic was placed at ~18 At.% C and 2690°C (O. Ruff and R. Wunsch[28], 1914), ~19 At.% 2475° (W. P. Sykes[12], 1930), 2732° (M. R. Nadler and C.P. Kempter[36], 1960), 25 At.% C and 2710°C

(R. T. Doloff and R. V. Sara[4, 5], 1960). The W_2C-WC eutectic was said to be located at ~42 At% C and a temperature of 2525°C[12].

There is general agreement that the solid solubility of carbon in tungsten is very small (< 0.1 At%)[17].

Table 3. Melting Temperatures of Tungsten-Carbon Phases[17, 25] (Literature Data)

Phase	Melting or Decomposition Temperature, °C	Ref	Investigator
W_2C	2880°	32	Andrews, et.al. 1921
	2860 ± 50°	33	C. Agte, et.al., 1930
	2730 ± 15°	34	Barnes, 1929
	2750 ± 50°	12	Sykes, 1930
	2795°(30 At% C)	4, 5	Doloff and Sara, 1961
WC (dec.)	2650 ± 50°C	28	Ruff, et.al. 1941
	2780°C	32	Andrews, et.al. 1921
	2880°C	35	Friedrich, et.al. 1925
	2870 ± 50°C	33	Agte, et.al., 1930
	2600°	(12)	Sykes, 1930
	2720°	36	Nadler, et.al. 1960
	2755°(peritectoid dec)	4, 5	Doloff and Sara, 1961

III. EXPERIMENTAL PROGRAM

A. STARTING MATERIALS

For the preparation of the experimental alloy material, the elemental powders as well as prealloyed tungsten monocarbide were used.

The tungsten powder (Wah Chang Corporation, Albany, Oregon) had the following impurities (contents in ppm): Mo-50, O-720 (1000*), Fe-40 (20), Ni-20 (< 50), N-n.d. (430), sum of other metallic impurities -< 60. The average grain size of the tungsten powder was 6.8 micrometers (Fisher subsieve); the lattice parameter, obtained from a Debye-Scherrer exposure with Cu-K_α radiation, was a = 3.1665±0.003 Å.

The spectrographic grade graphite powder (Union Carbide Corporation, Carbon Products Division) had the following analysis (contents in ppm): Sum of metallic impurities (Al + Cu + Mg + Si + Fe), and sulfur - < 100, ash-< 500 ppm, volatile matter-100 ppm. No second phase impurities were detected in the powder patterns. The lattice parameters found were a = 2.463 Å, and c = 6.729 Å, which compare favorably with literature values of a = 2.461 Å, and c = 6.708 Å [27].

The tungsten monocarbide was prepared by reacting well-blended and compacted stoichiometric mixtures of tungsten and carbide at temperatures varying between 1700 and 2000°C in a graphite tube furnace under hydrogen. After homogenization for approximately 2 hrs, the reaction product was allowed to cool under vacuum. The resulting cakes were then crushed and further comminuted to a grain size of < 40 micrometers by wet ball milling (acetone). After the powder was acid-leached in 5N hydrochloric acid to remove traces of cobalt and iron, picked up

*Numbers in the brackets refer to a check analysis made on the starting materials.

during the milling operation, the slurry was filtered and finally washed and dried. The carbide had a total carbon content of 6.15 Wt% C, from which 0.04 Wt% were present in free form. The lattice parameters obtained for this starting material are a = 2.906 Å, and c = 2.837 Å. Gas-fusion analysis performed to determine hydrogen, oxygen, as well as nitrogen, showed, that these impurities were present at a very nominal level (O + N + H < 80 ppm) only. No iron, nickel, or cobalt could be detected by sensitive spot-analysis after the acid-leach.

B. EXPERIMENTAL PROCEDURES

1. Sample Preparation and Heat Treatment

The bulk of the experimental alloy material was prepared by short-duration hot-pressing[3] of the well-blended mixtures of tungsten, tungsten monocarbide, and graphite. The resulting compacts were then surface-ground to remove the reaction layer (< 0.2 mm) and the adhering graphite skin, and then subjected to the homogenization treatments. The lower temperature (< 1800°C) heat-treatments were carried out in a tungsten-mesh-element furnace (R. Brew Company) under a vacuum of better than 10^{-5} Torr. To reduce carbon losses due to vaporization, equilibration treatments above 2000°C were carried out under high purity helium of ambient pressure. Typical heat-treatment schedules, employed for the prehomogenization treatments of the alloys, are listed in Table 4.

A number of alloys were prepared by sintering, and a few alloy buttons were arc melted under a high purity helium atmosphere.

Rapid quenching studies (Figure 5) were performed by dropping the sample from equilibrium temperature into a tin bath which was preheated to 300°C. To avoid interference from carburization zones, three wafers of the same sample material were inserted into the quenching furnace, from which only the center slab was subjected to further evaluation.

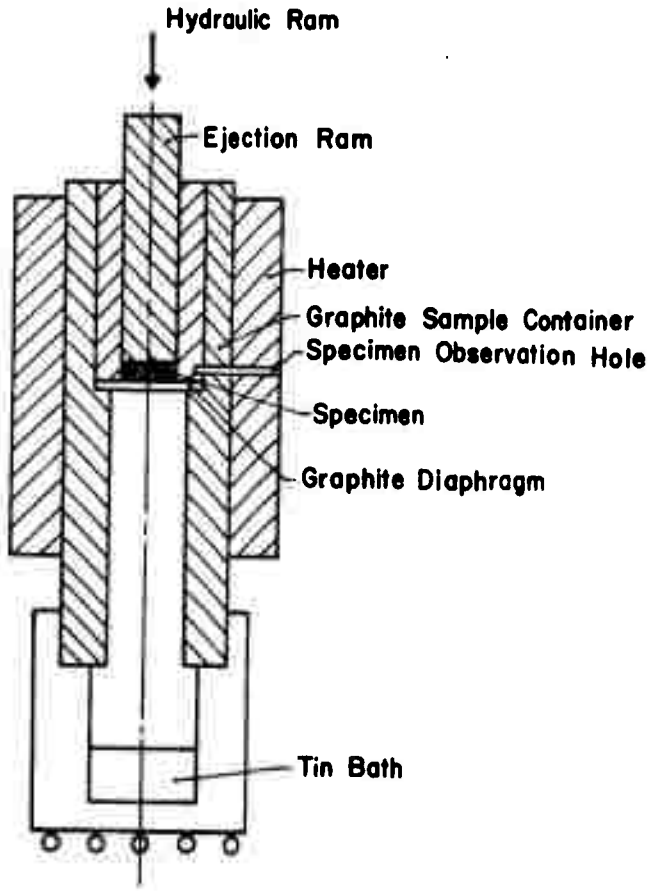

Figure 5. Experimental Setup for Rapid Quenching Studies on Carbides.

Table 4. Homogenization Treatments for Tungsten-Carbon Alloys

Temperature °C	Duration Hrs.
2400°C	3
2200°C	10
1800°C	46
1300°C	110
1190°C	165

2. Melting Temperatures and Differential-Thermoanalytical Studies

The melting points of tungsten-carbon alloys were measured with the previously described Pirani-technique[3, 42]. A small sample bar with a black body hole (~0.6 mm dia) in the center is heated resistively between two water-cooled copper electrodes to the temperature of the phase change. Melting is observed with a disappearing filament type micropyrometer. Pyrometer calibration and temperature correction data have been described in a previous report[3].

With the exception of tungsten, for which the melting point was determined also under vacuum, the final measurements on tungsten-carbon alloys were carried out under 1.3 atmospheres helium in order to avoid carbon losses due to vaporization.

In general it was experienced that the composition of the samples after melting did not deviate more than 0.5 atomic percent from the nominal composition. The precision of the temperature measurements in terms of the mean deviation in the individual measurements is a function of the melting behavior, but was in each case better than $\pm$ 10°C.

The temperature figures as noted in the figures refer to the precision of the measurements, and do not include the errors in the pyrometer calibration. The overall uncertainties of the temperature figures can be computed from the relation

$$\bar{\sigma} = \pm \sqrt{\sigma_m^2 + \sigma_c^2}$$

where $\bar{\sigma}$ denotes the overall temperature uncertainty, and σ_m and σ_c stand for the errors in the measurements and the pyrometer calibration, respectively. Respective values for σ_c are $\pm$ 10°C at 2300°C, $\pm$ 17°C at 3000°C, and $\pm$ 30°C (estimated) at 4000°C.

3. X-Ray Analysis

X-ray powder patterns with Cu-K_α-radiation were prepared from all alloys prepared in the course of the experimental investigations. The X-ray films were measured on a Siemens-Kirem coincidence scale.

High temperature (>2500°C) quenched alloys from the concentration region 34 to 45 At% C were run in the as-quenched state on a diffractometer using a scintillation counter, in order to avoid decomposition of the cubic high temperature phase during grinding for the normal X-ray powder analysis.

4. Metallography

The specimens were mounted in an electrically conductive combination of diallyl-phthalate-lucite-copper powder. After coarse grinding on silicon carbide paper (grit sizes varying between 120 and 600), the samples were mechano-chemically polished using a slurry of 0.05 micrometer alumina in diluted Murakami's solution. The polished surfaces were electroetched in a 2% aqueous sodium hydroxide solution. In order to achieve adequate etching of the higher carbon alloys (> 30 At%), a somewhat higher current level than used for excess tungsten-containing alloys was employed.

5. Chemical Analysis

Total and free carbon were determined using standard techniques. Oxygen, nitrogen, and hydrogen contents were analyzed employing the gas fusion technique; low level metallic impurities were determined in a semiquantitative way spectrographically.

C. RESULTS

1. Melting Point of Tungsten

Three melting point samples were prepared by cold-pressing the metal powder in steel dies. The green compacts were sintered for 1 hour at 1600°C under a vacuum of 5×10^{-6} Torr to acquire sufficient strength for the further processing. The specimens were then clamped between the two copper electrodes of the melting point furnace and held in position by two tungsten platelets (Figure 6). One sample was melted under vacuum, while the other determinations were run under 1.3 atmospheres of pure helium. A typical appearance of a melting point sample after the run is shown in

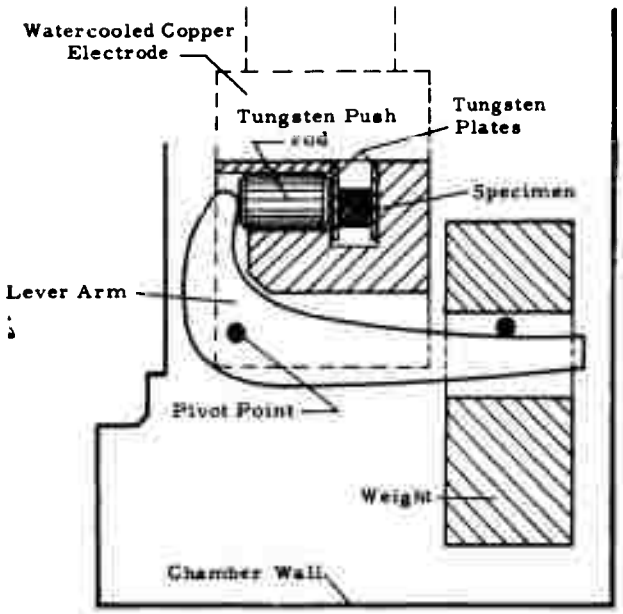

Figure 6. Specimen Clamping Device in the Melting Point Furnace.

Figure 7. From the measurements, a melting point of 3423 ± 10°C for pure tungsten was derived.

2. The Concentration Range W to W_2C

Alloys with nominal carbon concentrations of 0.5, 1.5, and 2.5 At% C, and which were quenched from 2600°C, were two-phased, containing needle-shaped W_2C in a homogeneous tungsten matrix (Figure 8). No phase other than the subcarbide were observed in heat-treated as well as in quenched alloys with carbon concentrations up to

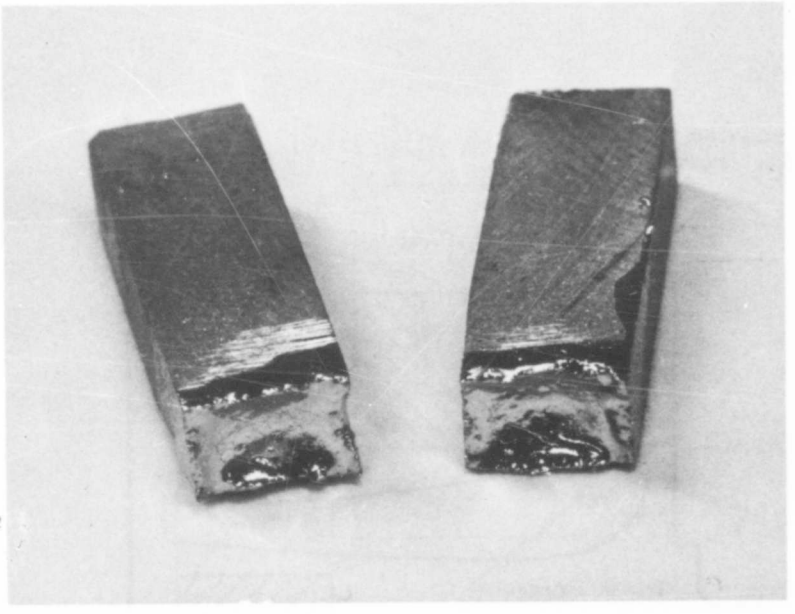

Figure 7. Tungsten Melting Point Specimen After the Run.

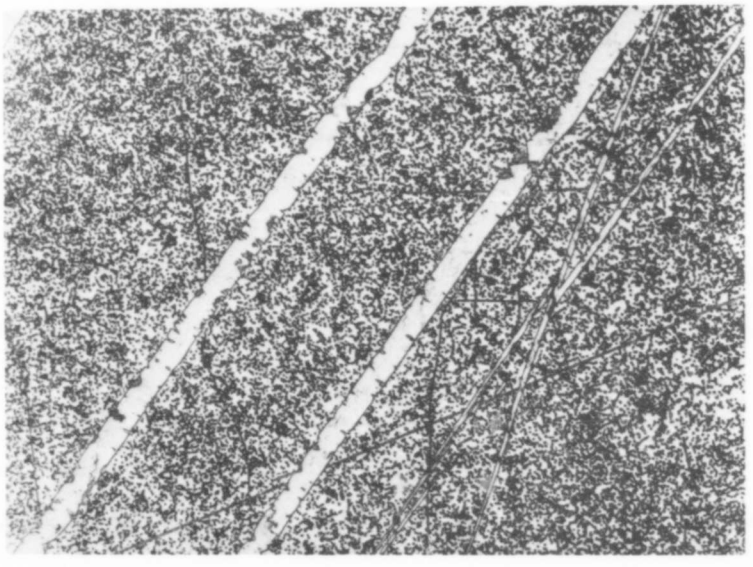

Figure 8. W-C (0.5 At% C), Melted, Re-equilibrated for 5 minutes at 2600°C, and Quenched. X250

Acicular W_2C and Tungsten (Covered with Etch-Pits)

29 At% C. Two-phase melting (Table 5) was observed for all alloys with less than 20 At% C. The specimens containing 20 and 24 At% C respectively, melted sharp, indicating that the eutectic point must be located between these compositions. Two phase melting was again noticed for alloys with carbon concentrations up to 28 At% C.

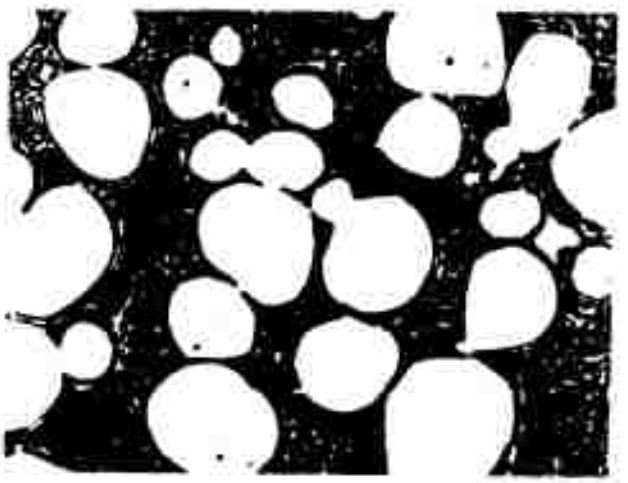

Figure 9. W-C (15 At% C), Cooled at ~80°C per Second from 2820°C. X1000

Primary Crystallized Tungsten in a W + W_2C Eutectic Matrix.

Metallographic examination of alloys with 15 and 20 atomic percent carbon showed primary crystallized tungsten in a matrix of W + W_2C eutectic (Figure 9), while the alloy with 24 At% C already contained approximately 50% primary W_2C.

The eutectic composition was bracketed by alloys with 21.5, 22, and 22.5 At% C, which were cooled from temperatures

slightly above the eutectic temperature (Figures 10, 11, and 12). Generally it was experienced, that cooling rates below 100°C per second had to be employed in order to allow the structure (lamellae spacing) to be resolvable by the light microscope.

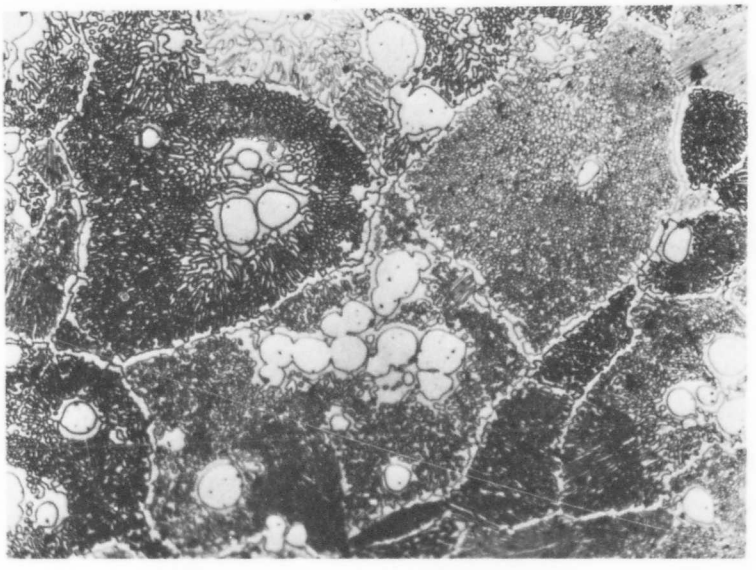

Figure 10. W-C (21.5 At% C), Quenched at ~80°C per Second from 2720°C . X500

Small Amounts of Primary Crystallized Tungsten in a $W + W_2C$ Eutectic Matrix.

The eutectic structure consists of fibrillous carbide embedded in a tungsten matrix (Figure 13 and 14), and the grains within a given eutectic colony have approximately the same orientation.

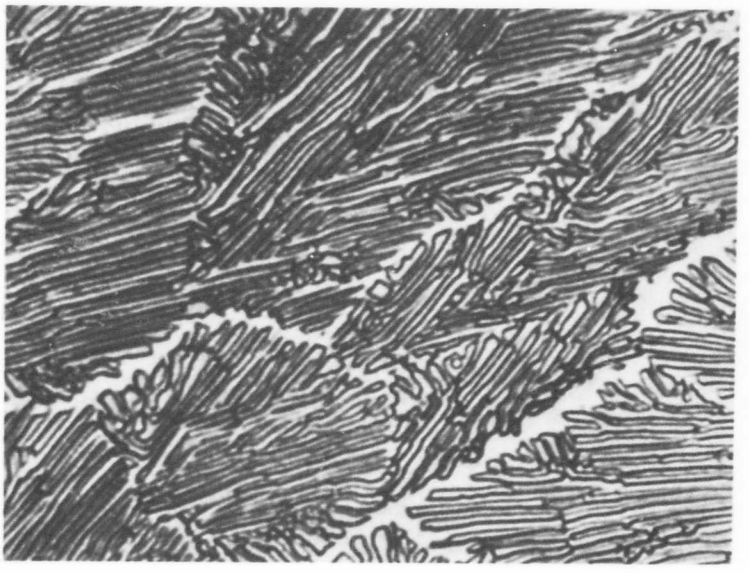

Figure 11. W-C (22 At% C), Quenched at ~ 80°C per Second from 2720°C. X2500

$W + W_2C$ Eutectic.

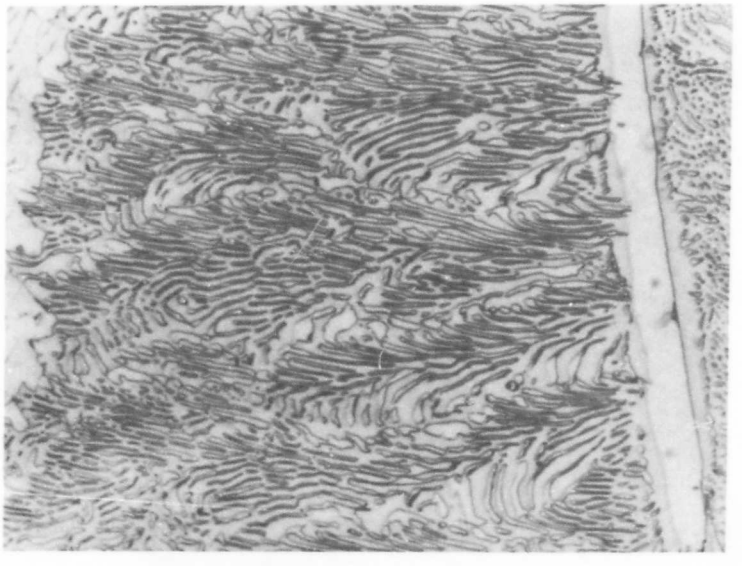

Figure 12. W-C (22.5 At% C), Cooled at 10°C per Second from 2730°C. X750

Small Amounts of Primary Crystallized W_2C in a $W + W_2C$ Eutectic Matrix.

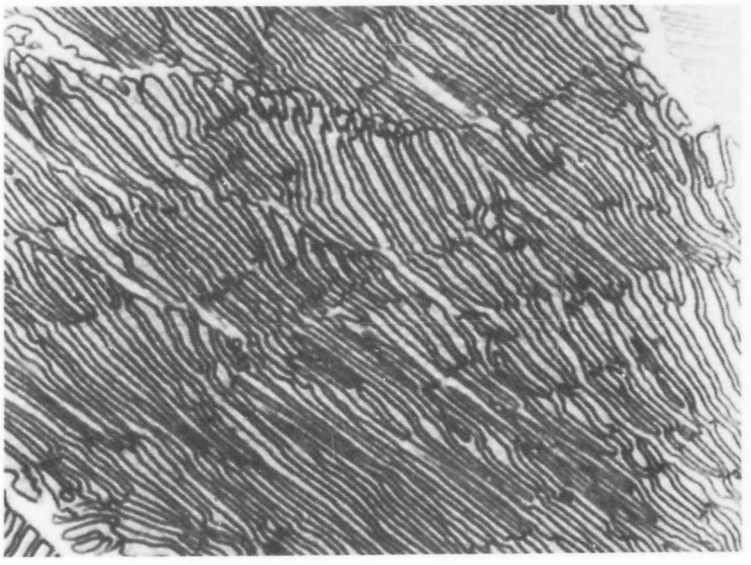

Figure 13. W-C (21.5 At% C), Quenched at ~80°C per Second from 2720°C. X2500

Preferred Orientation Within a Eutectic Colony W + W_2C (Longitudinal Section)

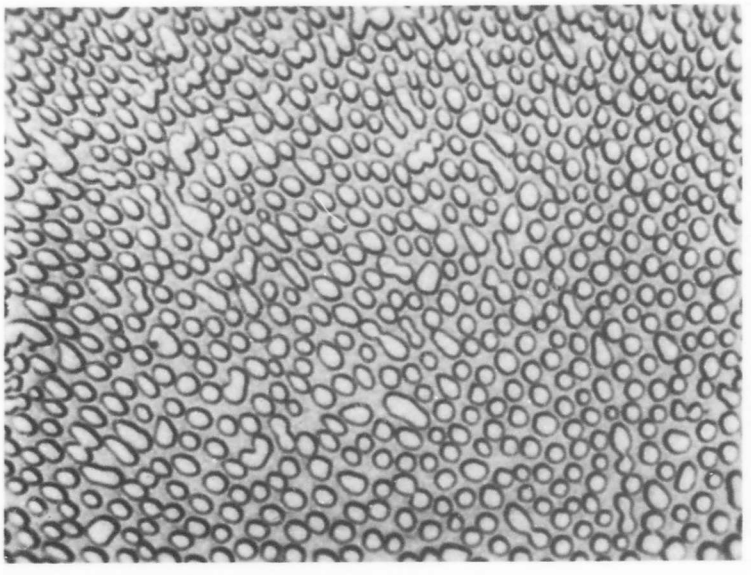

Figure 14. W-C (21.5 At% C), Quenched at ~80°C per Second from 2720°C. X2500

W_2C-Fibrillae in a Tungsten Matrix (Vertical Section).

3. The W_2C-Phase

Commencing at carbon concentrations of ~26 At% the melting temperatures of the alloys show a sharp increase (Table 5, Figure 15), maximizing at 2776 °C at a composition of 30 to 31 atomic percent carbon. The melting temperature of the stoichiometric composition already is about 25 °C lower than that of the congruently melting composition. Incipient melting in the concentration range from 34 to 37 At% C was observed at ~2735 °C, indicating that an isothermal reaction has been reached.

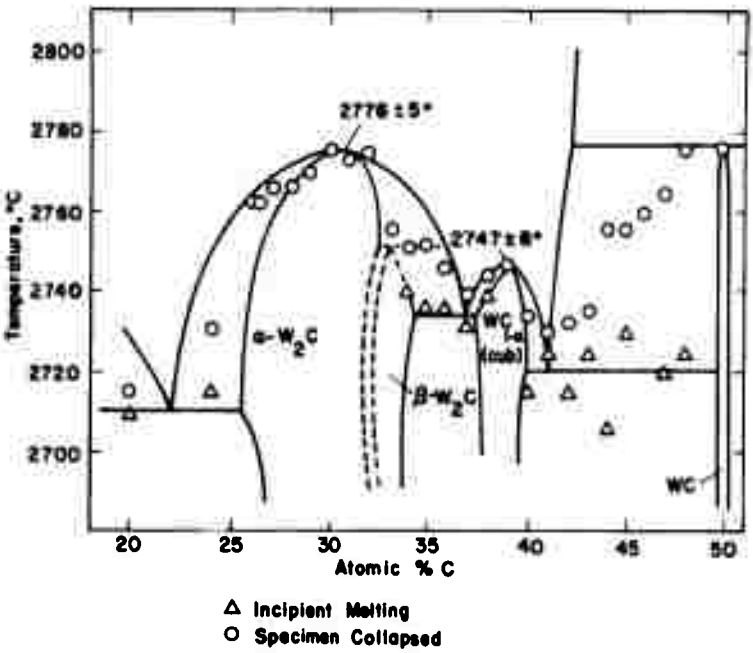

Figure 15. Tungsten-Carbon:Measured Melting Temperatures of the Alloys and Partial Phase Diagram.

Table 5. Melting Temperatures of Tungsten-Carbon Alloys

No	At% C Nom.	At% C Anal.	Number of Runs	Melting Temperatures, °C Incipient	Melting Temperatures, °C Collapsed	Cond	Melting
1			3	3423±10	3423±10	1	Sharp
2	10.0	10.0	1	2705	2900	1	Very Heterogeneous
3	15.0	-	1	2710	2820	1	Very Heterogeneous
4	20.0	20.1	2	2710±4	2715±4	1	Fairly Sharp
5	24.0	-	2	2714±5	2730±5	1	Fairly Sharp
6	26.0	26.3	2	2760±6	2763±4	1, 2	Slightly Heterogeneous
7	27.0	27.0	2	2766±6	2766±6	1, 2	Slightly Heterogeneous
8	28.0	28.1	2	2677±4	2766±4	1, 2	Fairly Sharp
9	29.0	29.0	2	2770±5	2770±5	1, 2	Fairly Sharp
10	30.0	30.2	2	2776±4	2776±4	1	Fairly Sharp
11	31.0	-	1	2773	2773	1	Fairly Sharp
12	32.0	32.0	4	2777	2777	1, 2	Fairly Sharp
13	33.0	33.15	2	2756+7	2756+7	1	Fairly Sharp
14	34.0	-	2	2740±3	2751±7	1	Slightly Heterogeneous
15	35.0	-	2	2736±5	2752±6	1	Heterogeneous
16	36.0	36.2	3	2736±4	2740±7	1	Sharp
17	37.0	37.3	4	2731±4	2739±4	1	Sharp
18	38.0	-	1	2739	2744	1	Sharp
19	39.0	-	2	2748+8	2748+8	1	Sharp
20	40.0	40.0	2	2715±8	2734±4	1	Slightly Heterogeneous
21	41.0	41.1	3	2725±4	2730±7	1, 2	Sharp
22	42.0	-	2	2715±5	2732±5	1	Slightly Heterogeneous
23	43.0	-	3	2725±4	2735±7	1	Slightly Heterogeneous
24	44.0	-	2	2705±7	2756±10	1	Alloys melt very
25	45.0	-	3	2730±4	2756±10	1	heterogeneously;
26	46.0	-	2	-	2760±10	1	melt exudes from
27	47.0	-	1	2720	2765	1	the samples, leaving
28	48.0	-	3	2725+5	2776+3	1	a porous graphite
29	50.0	49.9	3	-	2776±10	1	skeleton as remainder
30	53.0	-	1	-	2780	1	
31	56.0	-	1	2777	2820	1	
32	60.0	-	1	2777	2820	1	
33	65.0	-	1	-	2860-3350	1	

Legend to Table 5.

1. 1.3 atm He
2. 10 Torr, 5 cfh He-flow

The low carbon-boundary of the phase at the $W + W_2C$ eutectic temperature extends to ~25.6 At% C, as evidenced by microscopic inspection of the corresponding alloys (Figures 16 and 17). Precipitation of tungsten in alloys with carbon contents up to 29 At% occurs extremely fast and could not be prevented by quenching (100°C to ~1000°C per second). The precipitations are unidirectional, and analogous to the dissolution reactions found for the corresponding phases in the Mo-C[3] and Ta-C system[2, 43]. Single Phase structures in the high temperature(> 2600°C)-quenched alloys were observed up to carbon concentrations of 32 At% (Figure 18).

An interesting behavior, however, was noticed in the alloys with slightly higher carbon concentrations: In addition to the unidirectional precipitation structure, (Figure 19) the development of a further, veinlet-type, substructure was noticed. The initial suspicion that these substructures might stem from microcracks which had formed during cooling and which were then augmented by the etchant could be rejected on the basis of subsequent diffusion couple studies. Similarly, the assumption that the observed transition structure might be due to the decomposition of the cubic high temperature phase could be discarded, since the B1-phase is separated by sharp boundaries from the W_2C (Figure 20). Initiation and progress of the reaction is more clearly depicted in the micrographs of quenched alloys (Figures 21 through 23).

While the reaction can be more readily followed at the carbon-rich boundary of the W_2C phase, a positive differentiation, whether

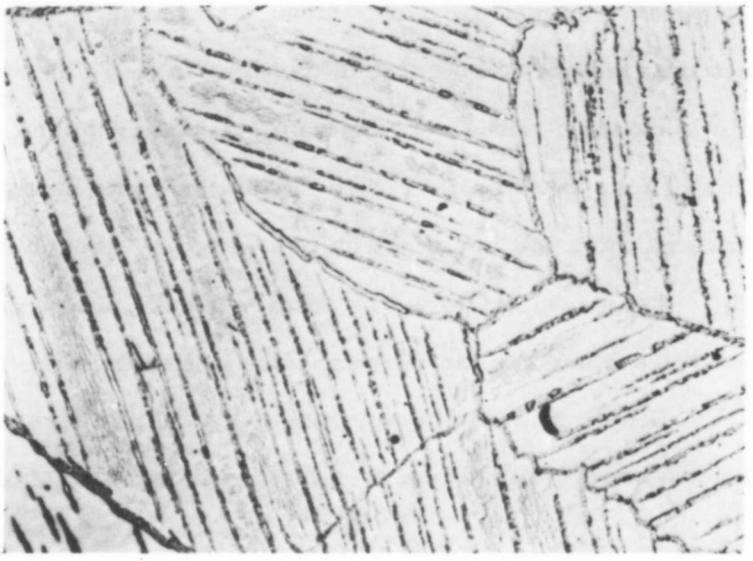

Figure 16. W-C (25 At% C), Quenched at ~50°C per Second X400 from 2720°C.

W_2C with Unidirectional Tungsten Precipitations, and Small Amounts of Excess Tungsten (W_2C-Depleted Eutectic) at the Grain Boundaries.

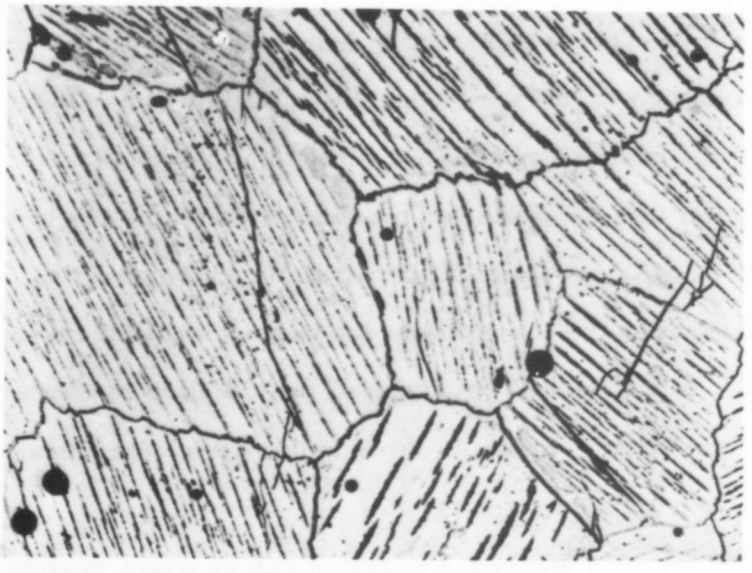

Figure 17. W-C (26 At% C), Quenched at ~80°C per Second from 2740°C. X400

W_2C with Tungsten Precipitates Formed During Cooling Pores (Black).

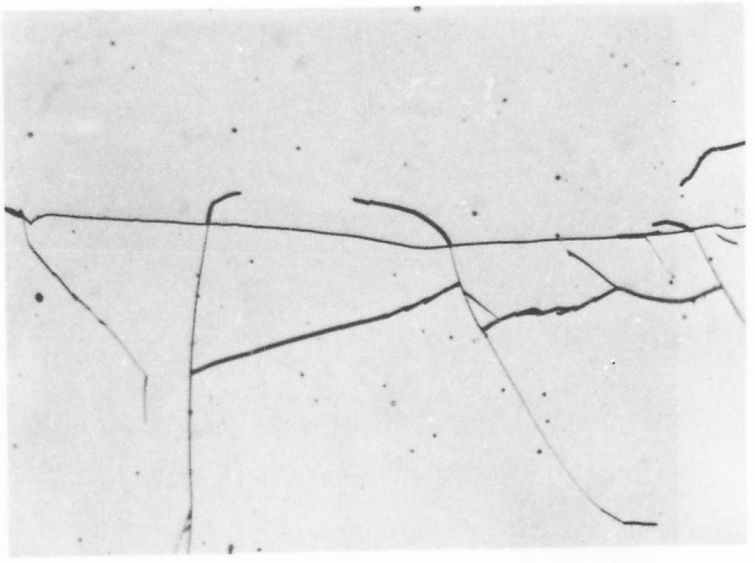

Figure 18. W-C (31.5 At% C), Rapidly Cooled (~ 10°C per Second) from 2760°C. X500

Single Phase W_2C.

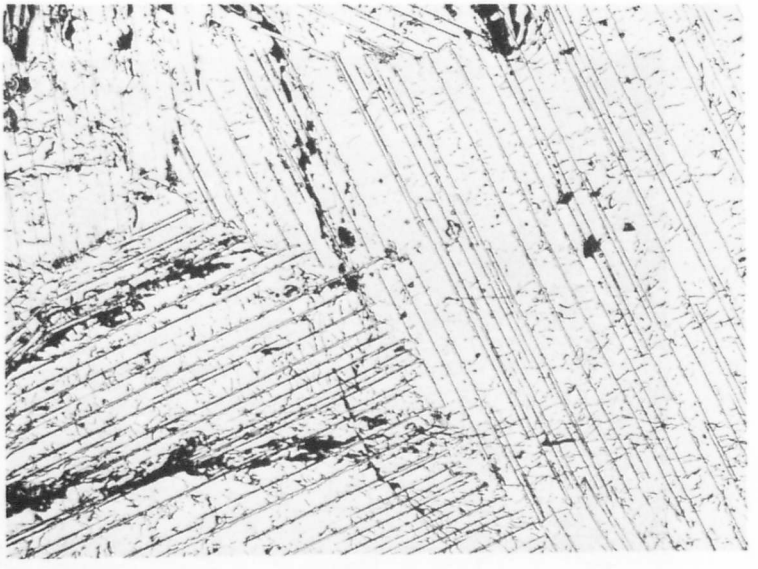

Figure 19. W-C (~ 33.5 At% C), Quenched at ~ 40°C per Second from 2420°C. X250

W_2C with Unidirectional Precipitations.
X-ray: W_2C with Traces of WC.

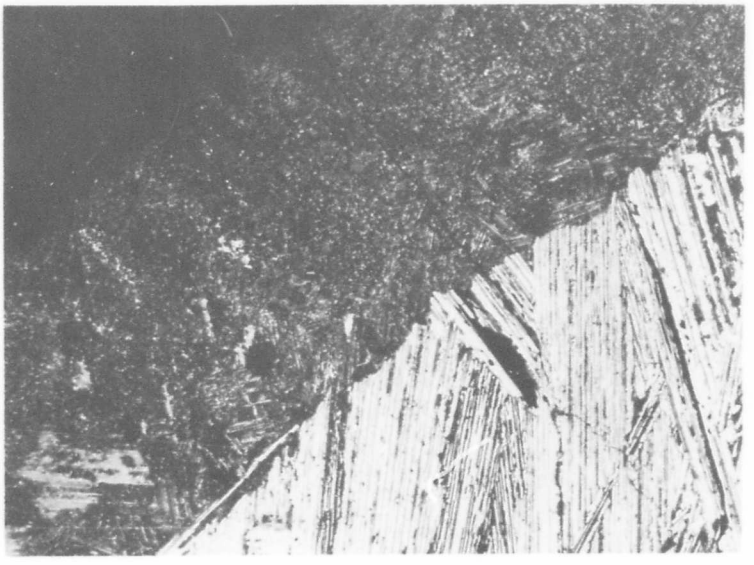

Figure 20. Diffusion Couple (W + 32 At% C)--Graphite (10 Minutes at 2680°C, Radiation-Cooled) X100

Outer Zone (Dark): Decomposed α-WC_{1-x} (B1)
Inner Zone : Precipitation + Transformation Structure of W_2C.

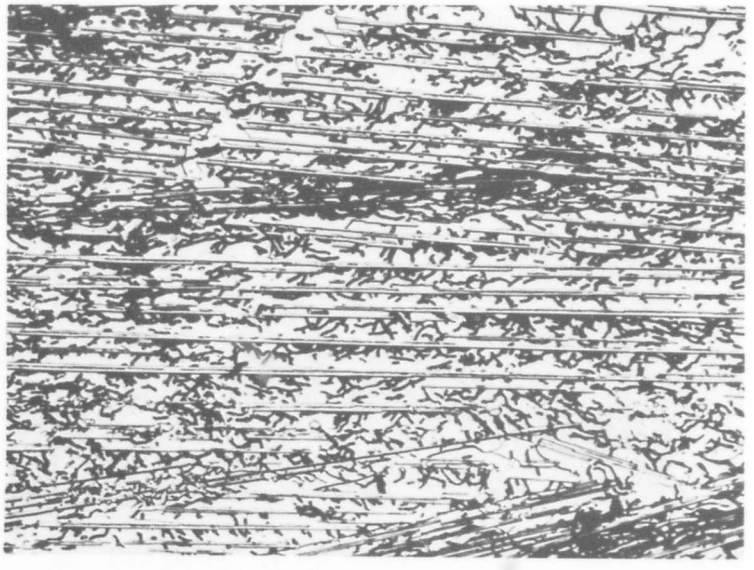

Figure 21. W-C (33.5 At% C), Quenched at ~100°C per Second from 2650°C. X250

Unidirectional Precipitations in W_2C, and Initiation of Eutectoid Decomposition of the β-W_2C.

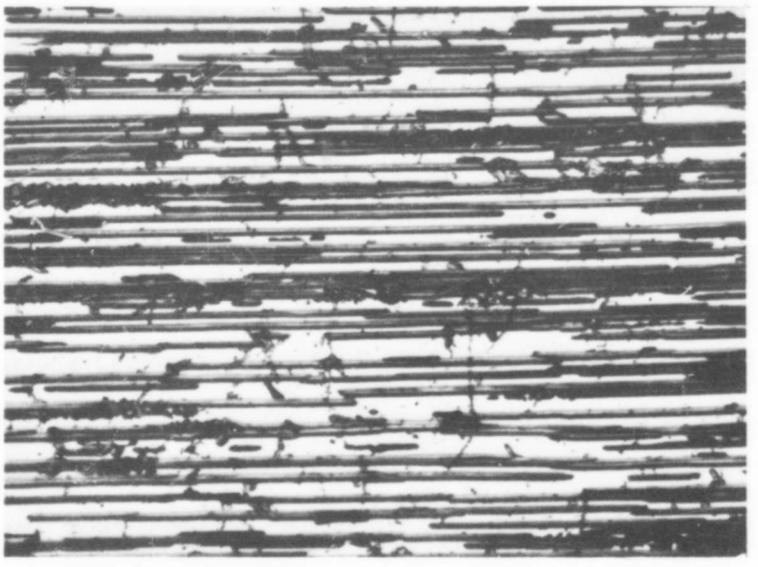

Figure 22. W-C (34 At% C), Quenched ~400°C per Second from 2600°C. X600

W_2C with Precipitations, and Initiation of the $\beta \rightarrow \alpha$-W_2C Phase Reaction.

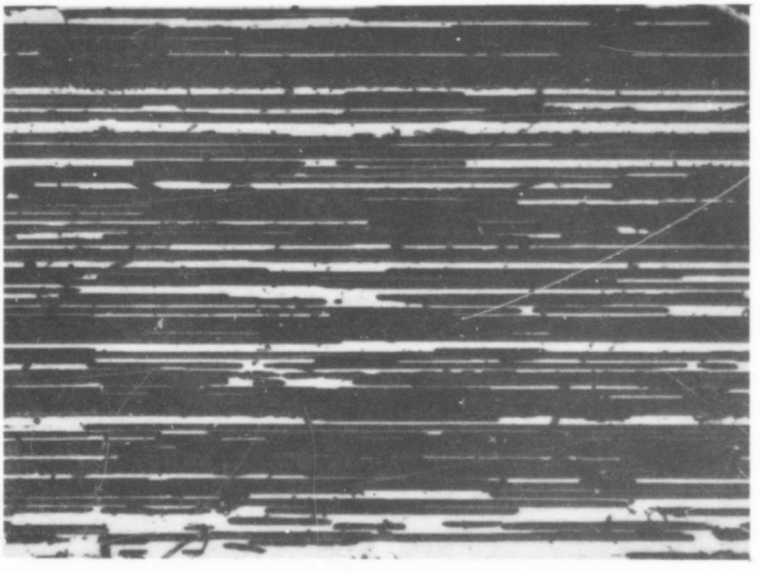

Figure 23. Specimen from Figure 22, Annealed with ~ 60°C per Second. X600

W_2C with Precipitations. β-α-W_2C Phase Reaction in an Advanced State.

the α-β-W_2C phase reaction proceeds single phased, or whether the β-phase is separated by a two-phase field from the α-phase, was more difficult to achieve. Carburization was in many instances nonuniform, resulting in uneven phase boundaries. Nevertheless, the evidence gained from a large number of experiments performed on alloys from the concentration range from 31 to 33 atomic percent carbon, strongly supports a two-phased reaction process. In the micrographs shown in Figures 24 and 25, it should be especially noted, that the unidirectional

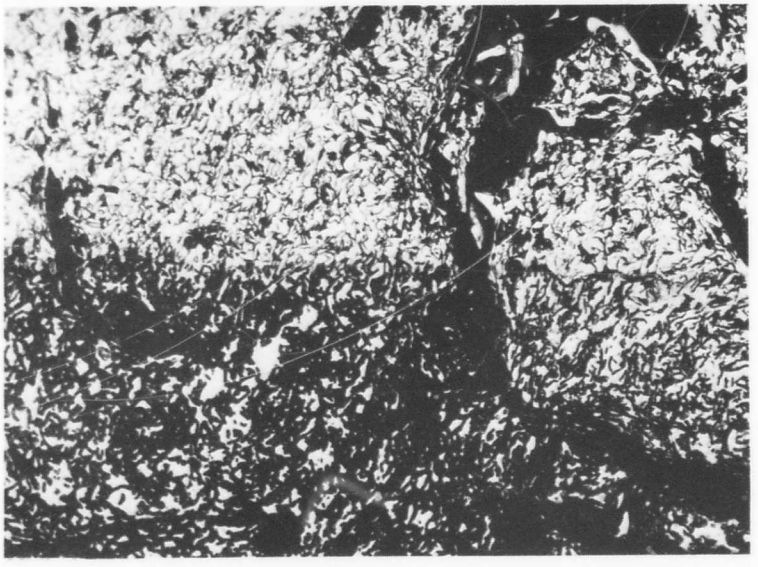

Figure 24. Diffusion Couple (W-32 At% C) -Graphite X150
10 Minutes at 2680°C, Radiation-Cooled

A: α-W_2C ($\sim$ 32 At% C)

B: β-W_2C (nearly completely decomposed)

X-ray: (A and B) : W_2C.

(α-WC_{1-x}) precipitations, characteristic for slightly hyperstoichiometric compositions, are absent, while the veinlet-type structure, previously assumed to represent the α-β-W_2^*C transformation structure, still prevails.

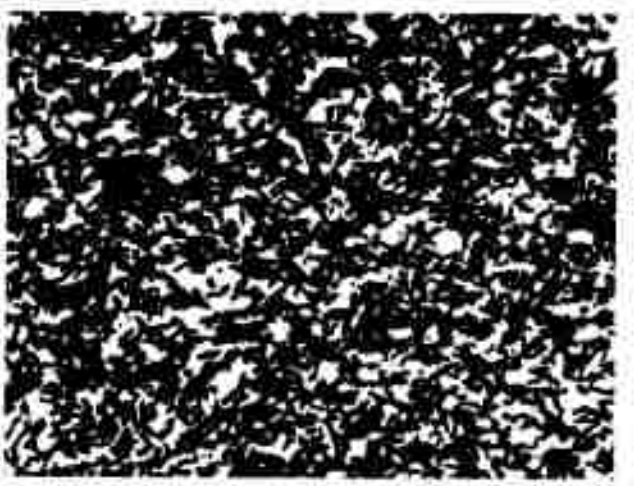

Figure 25. Enlarged View of the β-W_2C Region of the Sample Shown in Figure 24. X250

In order to obtain additional evidence for the reaction behavior of the W_2C phase, DTA-investigation on duplicate series of samples which covered the concentration range from 28 to 35 At% C, were performed.

No isothermal enthalpy changes were observed in alloys with carbon concentrations less than 32 At% (Figure 26). In the alloy with 33 atomic percent carbon (Curve B in Figure 26), an isothermal phase reaction at 2450°C is indicated, while still another arrest, occurring at somewhat higher temperatures, is observed in the alloy with 34 atomic percent (Curve D in Figure 26).

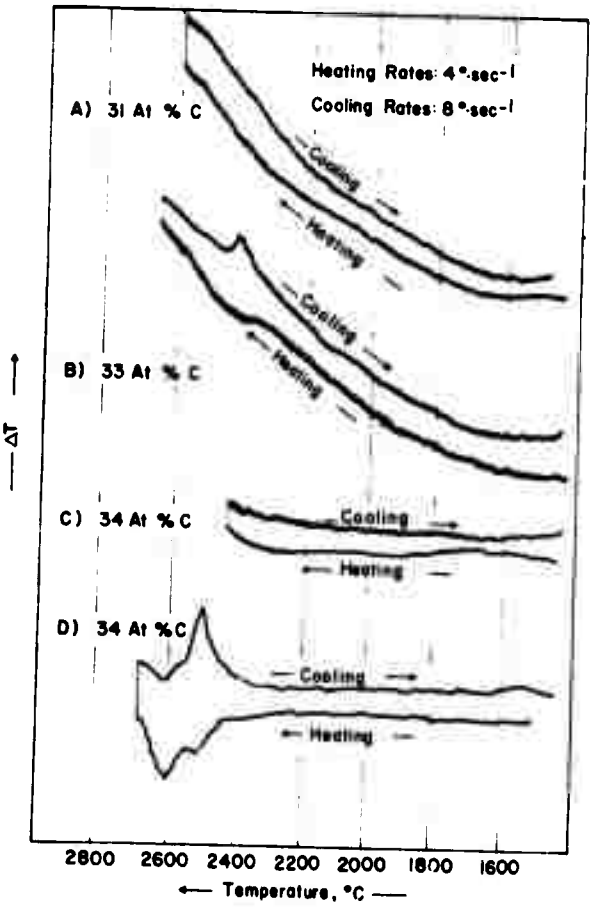

Figure 26. DTA-Thermograms of Tungsten-Carbon Alloys. Concentration Range 31 to 34 Atomic Percent Carbon.

The later signal increases in size as the carbon concentration increases (Figure 27), and was identified as being associated with the formation (heating) or decomposition (cooling) of the cubic high temperature phase. DTA-studies performed under transient concentration conditions were in full confirmation of these results, thus assuring the definite existence of an isothermal reaction in stoichiometric W_2C at temperatures around 2450°C.

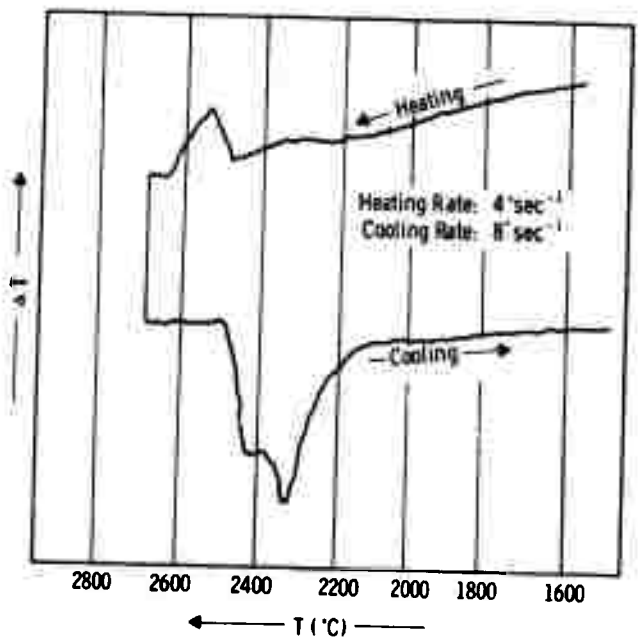

Figure 27. DTA-Thermogram of a Tungsten-Carbon Alloy with 35 Atomic Percent Carbon.

In summarizing our experimental evidence on the α-β-W_2C phase reaction, it has been established, that at the stoichiometric composition, the subcarbide undergoes an isothermal phase change at temperatures around 2450°C. The indications are, that the transformation proceeds as a two-phased (heterogeneous) reaction, with the metal host lattice remaining structurally unchanged. From the present results, the evidence gained in the investigation of ternary systems (Ta-W-C, W-Cr-C, Mo-Cr-C)[44], as well as from the existence of related reactions in other binary metal-carbon systems, we may deduce, that the transformation is of the second order and is associated with the destruction of long range order in the carbon sublattice. At substoichiometric compositions, disordering proceeds as a homogeneous reaction. It is yet uncertain, whether long range order can develop at all at significantly substoichiometric compositions; we therefore have to include the possibility, that the homogeneous disordering reaction ocurring at substoichiometric compositions may only involve a gradual change of short range order with temperature.

The variation of the lattice parameters of the W_2C-phase with the carbon content was measured on two alloy series which were rapidly quenched from 2200°C and 2400°C, respectively (Figure 28). According to the plot of the values obtained, (Figure 29) both lattice spacings decrease with increasing carbon defect. It may be mentioned in this connection, that a certain dependence of the lattice parameters upon the quenching temperature was noticed; this effect may be related to partial quenching of a less-ordered state prevailing at high temperatures.

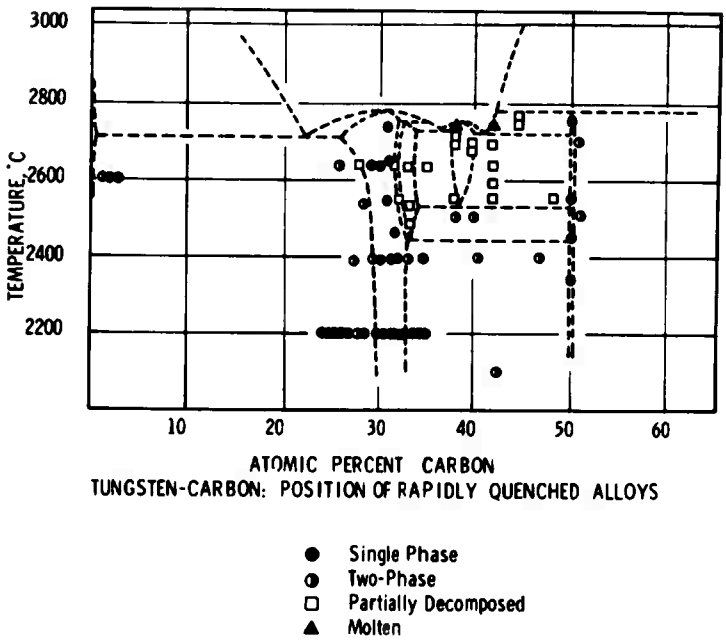

Figure 28. Tungsten-Carbon: Position and Qualitative Evaluation of Rapidly Quenched Alloys.

In order to study the possible decomposition of W_2C towards lower temperatures, single phase W_2C as well as alloys from the two-phase fields W + W_2C and W_2C + WC were heat-treated for 110 hrs at 1300°C, and for 165 hours at 1190°C. Whereas no detectable decomposition or change of the relative amounts of the phases was noticed in the 1300°C-treatment, detectable amounts of tungsten and tungsten monocarbide had formed in originally single-phased W_2C alloys after the treatment at 1190°C. This finding is in confirmation of previous claims[20], that W_2C is unstable below ~1250°C.

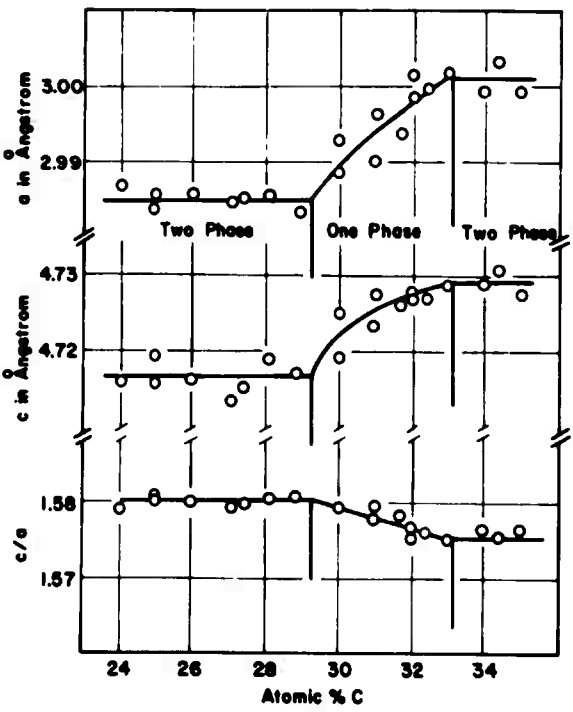

Figure 29. Lattice Parameters of W_2C.
(Alloys Quenched from 2200°C)

4. The Cubic High Temperature Phase (α-WC_{1-x})

DTA-investigations performed on alloys from the concentration range 34 to 43 At% C revealed the existence of a solid state reaction at temperatures around 2500°C (Figure 30 through 32). While in the DTA-thermogram of an alloy with 35 At% C(Figure 27) the

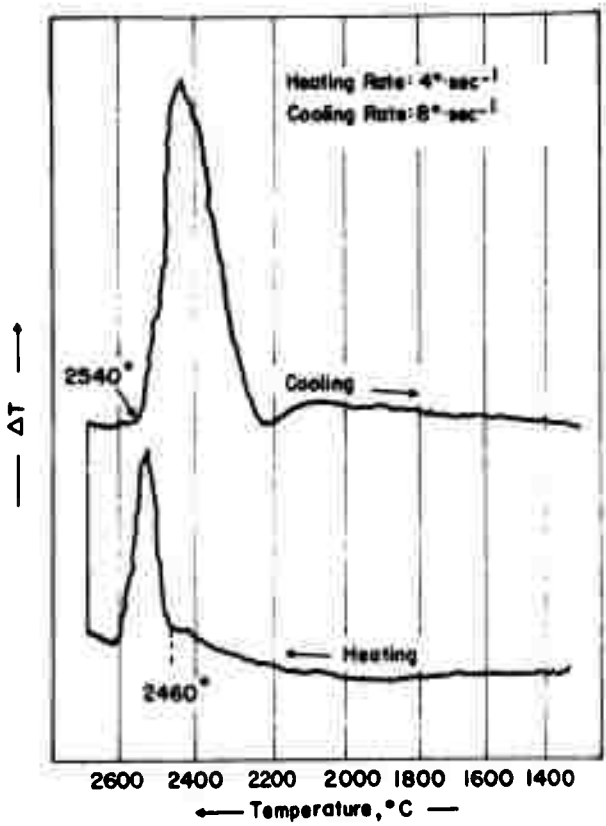

Figure 30. DTA-Thermogram of a W-C Alloy with 36 Atomic Percent Carbon.

peak due to the α-β-W_2C reaction is still clearly visible, the thermal arrest due to this reaction is gradually supplanted by the increasing intensity of the α-WC_{1-x} peak; it could not be distinguished from the background, once the carbon content exceeded 38 atomic percent.

The observed temperatures for the formation (heating) and decomposition (cooling) of the cubic tungsten carbides are practically

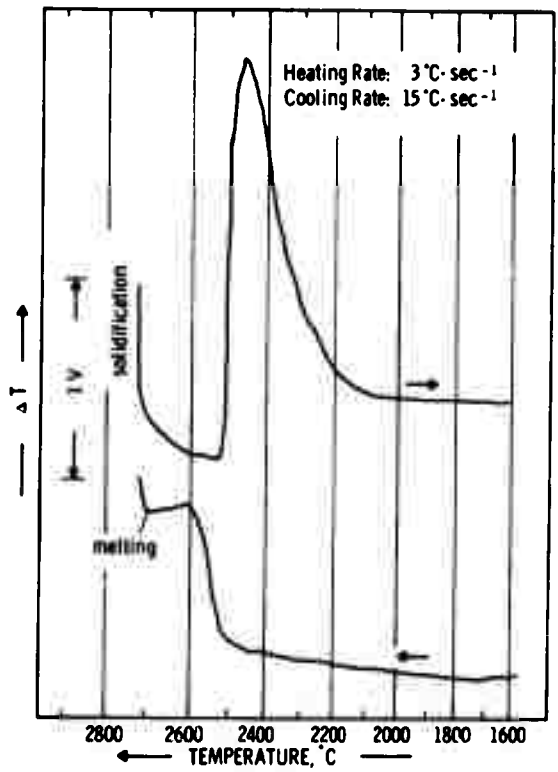

Figure 31. DTA-Thermogram of a W-C Alloy with 38 Atomic Percent Carbon.

independent of the heating and cooling rates (0.2 to 16 °C per second), indicating, that the underlying reaction proceeds with high speed. Rapid quenching of the alloys was only partially successful, since the cubic high temperature phase never could be retained in pure form, and was always accompanied by varying amounts of W_2C and WC. The lattice parameter of the cubic phase, determined from a diffractometer run on

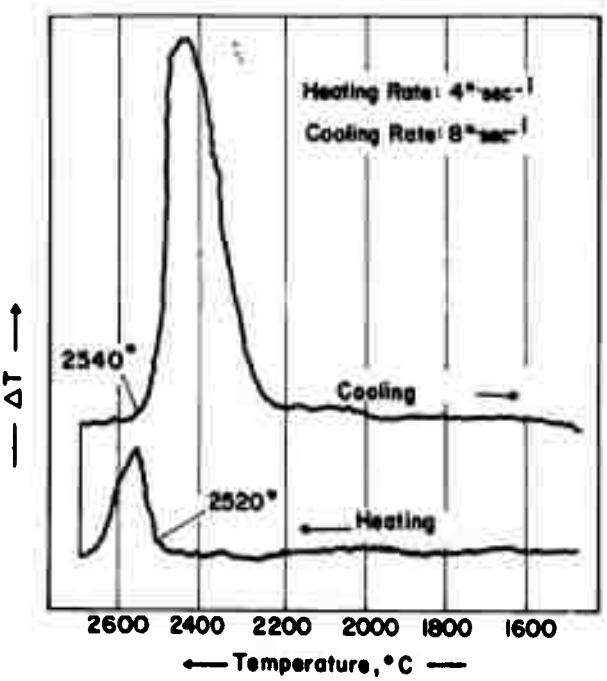

Figure 32. DTA-Thermogram of a W-C Alloy with 43 Atomic Percent Carbon.

an alloy with 38 At% C, and which was quenched from 2650°C, was $a = 4.220 \pm 1$ Å. No significant changes of the lattice dimensions of the phase with the carbon concentration or the quenching temperatures could be detected.

Metallographic examination of heat-treated as well as solid state quenched specimens were in confirmation of the DTA-results, and also showed the eutectoid point to be located closely to 38 At% C (Figure 33 through 35). In all these samples, tungsten monocarbide can be easily differentiated by its bluish-grey appearance, in contrast to W_2C and α- WC_{1-x}, which are much brighter in appearance.

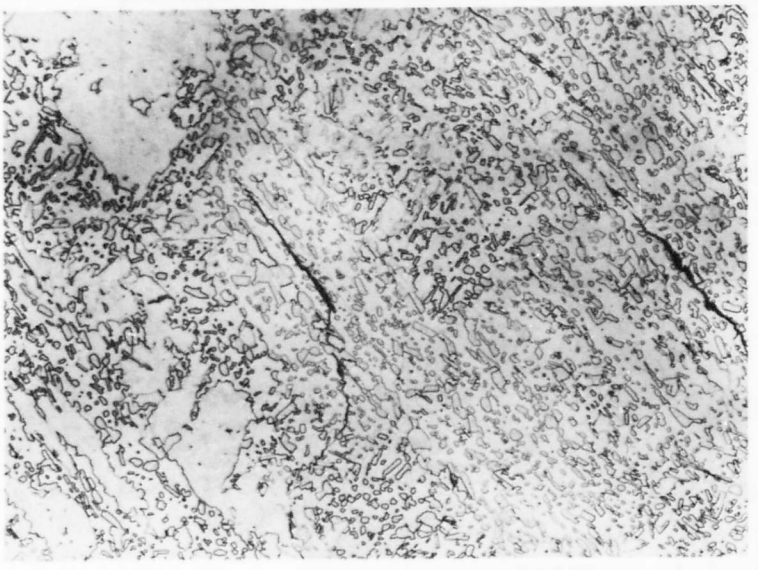

Figure 33. W-C (37.5 At% C), Quenched from 2400°C. X250
X-ray: W_2C + WC

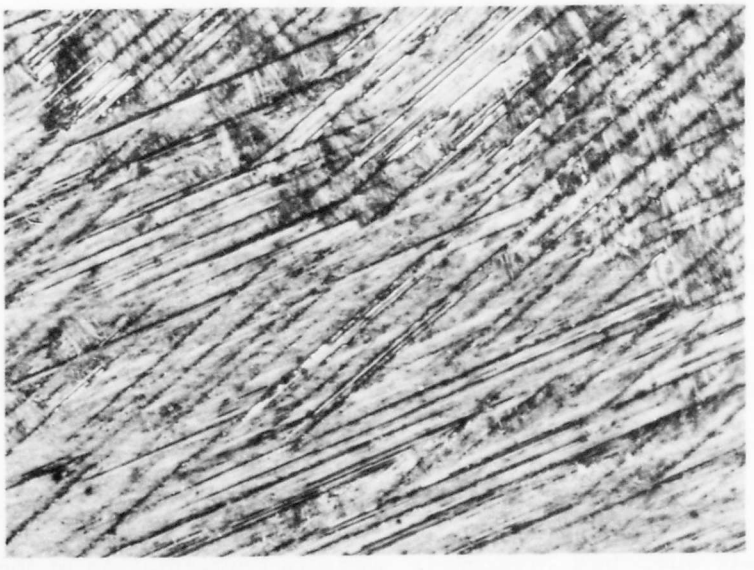

Figure 34. W-C (38 At% C), Rapidly Quenched (>500°C per Second) from 2580°C. X750

Partially Decomposed α-WC_{1-x}, with Traces of Excess WC.
X-ray: α-WC_{1-x}, Accompanied by Smaller Amounts of W_2C and WC.

Figure 35. W-C (38 At% C), Cooled at 2°C per Second from 2650°C. X750

Partially Reannealed Decomposition Structure of α-WC_{1-x}.

X-ray: W_2C + WC.

Alloys in the concentration range from 33 to 36 At% C, which were quenched from liquidus temperatures show primary crystallized W_2C in a eutectic structure (Figure 36). An alloy with 36.5 At% C was purely eutectic (Figure 37). Although not very pronounced, the melting temperatures indicate a melting point maximum for the cubic phase at ~2740°C and a composition around 39 At% C (Table 5 and Figure 15). A melting specimen showing the typical characteristics of congruent melting is shown in Figure 38.

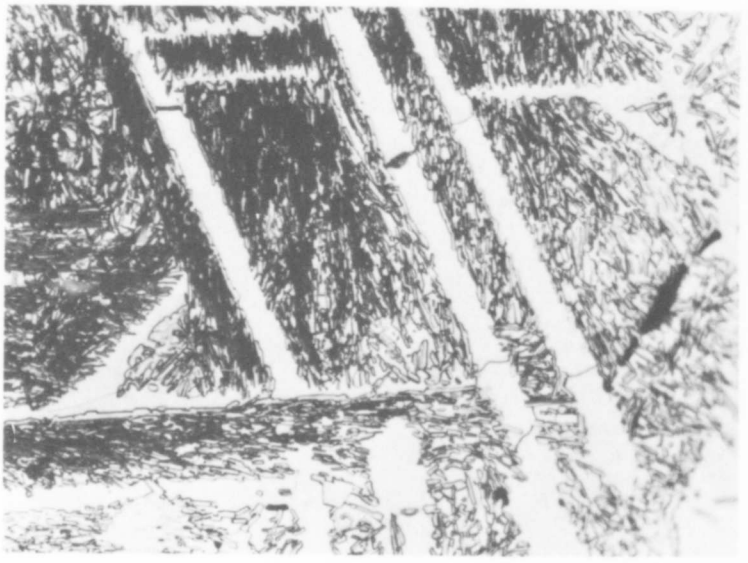

Figure 36. W-C (35.5 At% C), Cooled at ~ 20°C per Second from 2750°C. X750

Primary W_2C and W_2C + α-WC_{1-x} Eutectic.

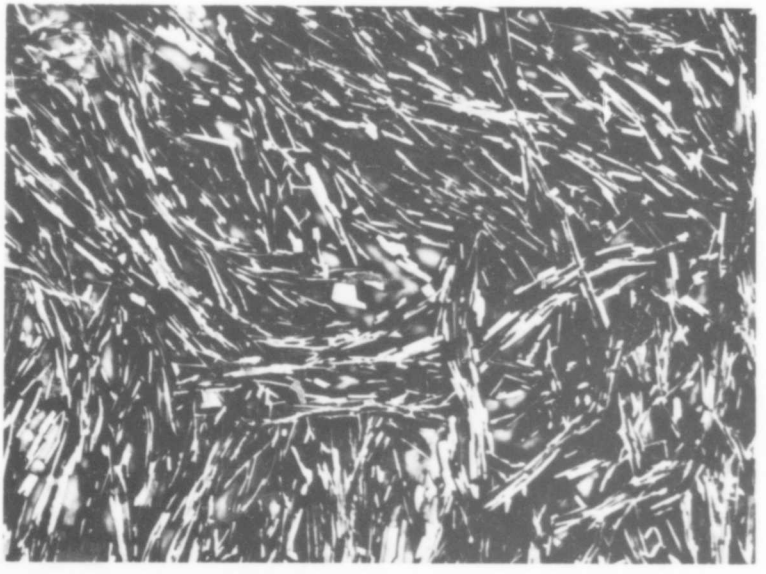

Figure 37. W-C (36.5 At% C), Quenched from 2750°C. X750

W_2C + α-WC_{1-x} Eutectic.

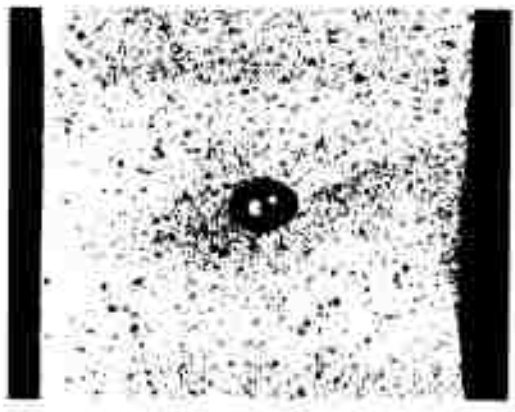

Figure 38. Center Portion of a Pirani Melting Point Specimen [W-C (61/39)] After Melting.
Note Black Body Hole Filled with Liquid.

5. The Concentration Range α-WC_{1-x} — WC, and the Monocarbide Phase

DTA- as well as melting point determinations on alloys from the two-phase range α-WC_{1-x}-WC showed incipient melting to occur at temperatures around 2720°C (Table 5, Figure 15, 39 and 40). The eutectic must be located closely to the cubic α-WC_{1-x} phase, since melting of somewhat higher carbon alloys occurs extremely heterogeneous, i.e. a wide gap is observed between the incipient melting temperatures and the temperatures at which the black body holes gradually closed. The final collapse of the specimens usually was preceded by an infiltration of the solid skeleton (WC) with the lower melting W_2C + WC eutectic. These findings are in essential agreement with the metallographic results (Figure 41).

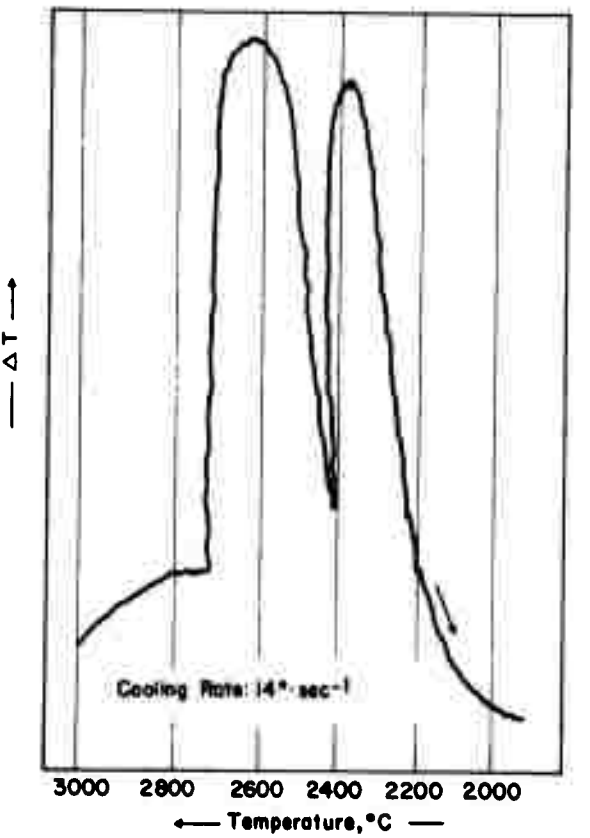

Figure 39. DTA-Thermogram of a W-C Alloy with 43 Atomic Percent Carbon.

Note Partial Superposition of the Solidification Peak and the Thermal Arrest Due to the Decomposition of α-WC_{1-x}.

No signs of a thermal arrest, which could be associated with a solid state (peritectoid) decomposition of WC could be found. However, once the peritectic temperature had been passed in an experiment, lower solidification temperatures, as well as the appearance

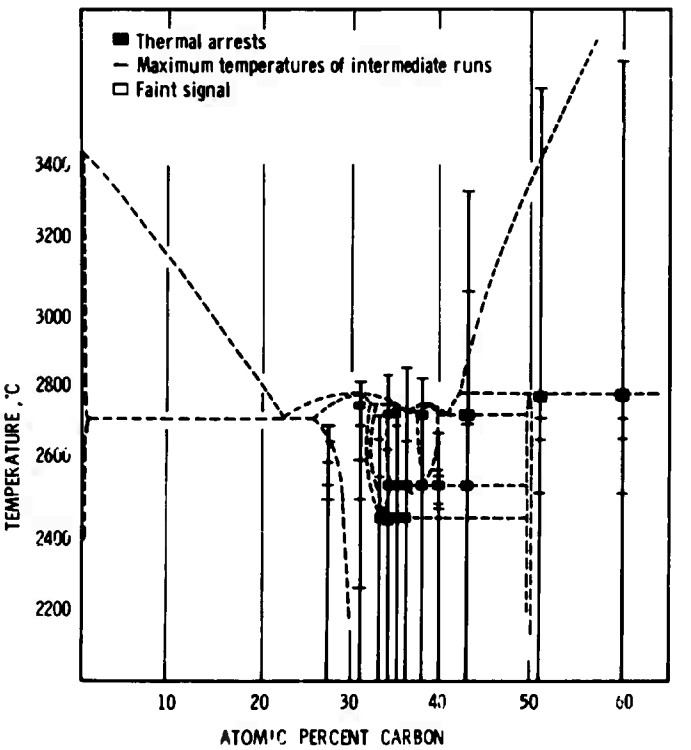

Figure 40. Summary of Differential-Thermoanalytical Investigations in the Tungsten-Carbon System.

of the peak for the α-WC_{1-x} decomposition reaction was noticed (Figure 42). Post-experiment examination of the alloys revealed a practically complete segregation of the higher density melt from the graphite, which had formed in the decomposition process (Figures 43 through 45). This also explains the rather gradual temperature arrest in the DTA-curves shown in Figure 42. Due to the physical separation of graphite and metal-rich

Figure 41. W-C (42 At% C), Quenched from 2730°C X400
α-WC_{1-x} + WC Eutectic, with Traces of Primary Crystallized Tungsten Monocarbide (Light).

melt, complete back reaction to WC within feasible lengths of time does not occur, i.e. analysis of as-melted WC-specimens and also of slowly cooled samples always will reveal a mixture of W_2C, WC and C.

6. High-Temperature Equilibration Experiments with Graphite

The presence of only small amounts of free graphite in the exuded melt from the WC-sample (Figure 45) indicated only a nominal compositional change of the liquidus curve with the temperature.

For a more accurate determination of the peritectic composition as well as the composition of carbon-saturated-tungsten-carbon melts at the hyperperitectic temperatures, an experimental arrangement as shown in Figure 46 was used.

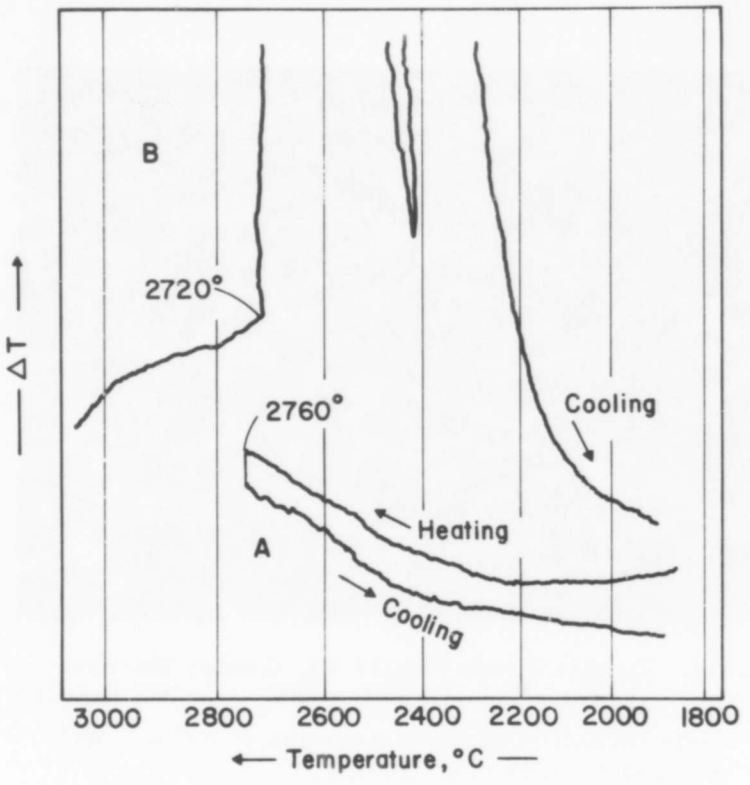

Figure 42. DTA-Thermogram of a Tungsten-Carbon Alloy with 51 Atomic Percent Carbon.

A. Without Prior Melting
B. After a Short Time Exposure to 3000°C.

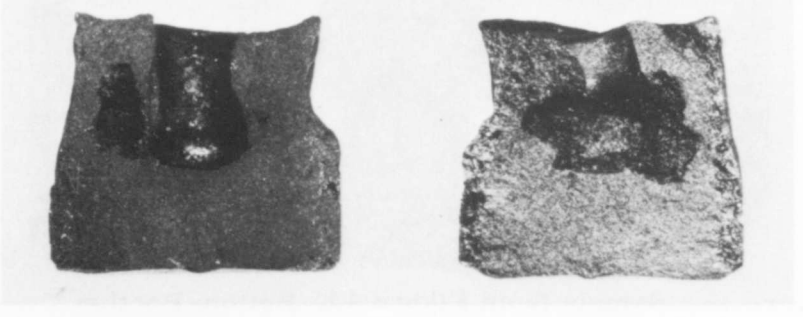

Figure 43. Segregation of Tungsten-Carbon Melts from Graphite: Appearance of an Originally Cylindrical DTA-Sample with 51 Atomic Percent Carbon After Partial Melting at 2800°C.

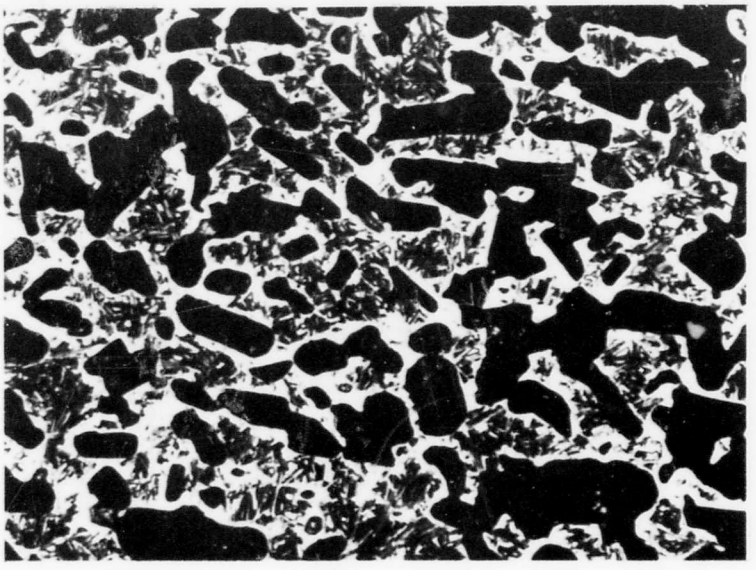

Figure 44. Sample From Figure 43, Center Portion X400
Graphite (Black) and α-WC_{1-x} + WC Eutectic.
Note Initiation of Back Reaction P + C —— WC
Around the Graphite Grains.

Figure 45. Sample from Figure 43, Bottom Portion X750
Traces of Free Graphite, Primary Crystallized
Tungsten Monocarbide, and α-WC_{1-x} + WC Eutectic.

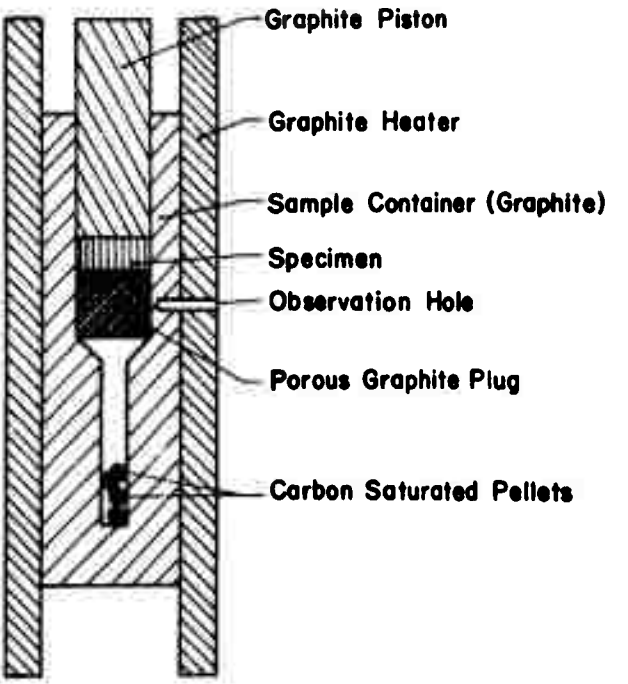

Figure 46. Experimental Arrangement for the Determination of the Composition of Graphite-Saturated Tungsten-Carbon Melts.

A porous cylindrical graphite plug was prepared by hot-pressing of graphite powder at temperatures around 2000°C, and was fitted into a graphite container with cylindrical bore. After placing the sample on top of the graphite plug, the cavity was closed by a graphite piston, and the whole arrangement inserted into a cylindrical graphite heater. The graphite element was resistively heated between two

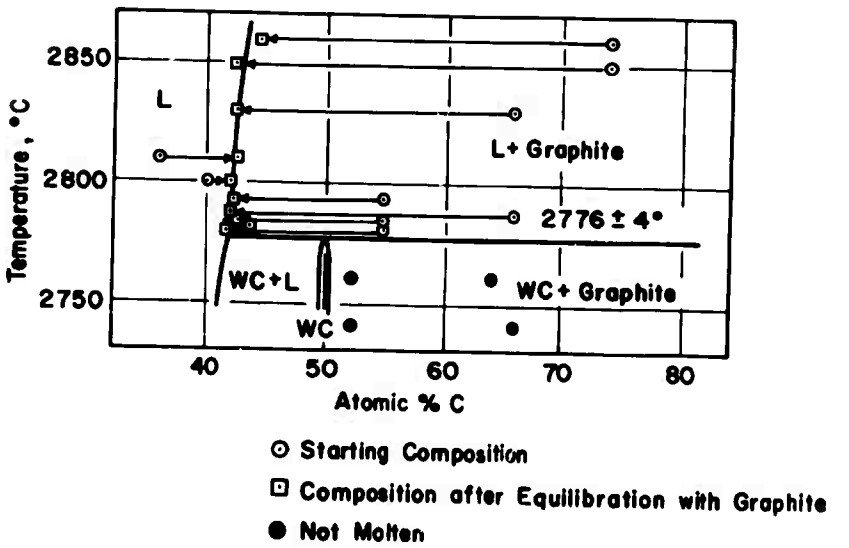

Figure 47. Tungsten-Carbon: Composition of the Peritectic Melt and the Liquidus Line Near the Decomposition Temperature of Tungsten Monocarbide.

graphite retainers, which were connected to two water cooled copper-electrodes. The temperature was measured pyrometrically through an observation hole drilled through the heater and through part of the sample container.

For the determination of the peritectic composition, the loaded container was slowly heated to the transition region, while a small force (~ 2 kg) was applied to the graphite piston. The melt formed at the peritectic temperature was then force-filtrated through the graphite plug, and was collected at the cooler end of the extended cylindrical channel, where it immediately solidified. The pellets were then chemically analyzed for their carbon content.

In order to assure that equilibrium had been attained in the experiments, the equilibrium state was approached from both sides, i.e. alloys which were either metal-or carbon-rich with regard to the equilibrium composition were used as starting components.

As a mean value from the measurements, a carbon concentration of 42 atomic percent was obtained for the peritectic liquid. The composition of the liquidus line changes only insignificantly towards higher ($\sim$ 2850 °C) temperatures (Figure 47).

The eq libration experiments at temperatures in excess of 2900°C were carried out somewhat differently, since it was observed, that the melted filtrated through the porous graphite plug even without application of external pressure. The sample container in the experimental arrangement shown in Figure 46 was made long eough to protrude from both ends of the heater, thus allowing to maintain a fairly large temperature gradient between the center portion and both ends. After bringing the container with the graphite plug to equilibrium temperature, the sample was admitted in small batches from the top. The melt formed at hyperperitectic temperatures gradually filtrated through the graphite plug, thereby assuming the equilibrium composition at the chosen temperature.

Check experiments performed showed, that the effective temperature drop of the system due to sample heat-up and melting was negligible, i.e. the heat capacity of the larger mass graphite plug as well as the re-approach rate of the equilibrium temperature were sufficiently high to keep the temperature changes at a negligible level.

It is essential, that the equilibrated melt is quenched to sub-solidus temperatures, in order to avoid falsification of the test results due to physical segregation of the graphite from the melt upon slow cooling. As mentioned earlier, rapid cooling conditions were achieved by letting the collecting channel protrude from the heating element. In this way, a temperature of 2100°C could be maintained during the equilibration cycle at the collecting end of the tube. A typical microstructure of an high-temperature equilibrated sample showing the homogeneous distribution of the primary crystallized graphite, is shown in Figure 48.

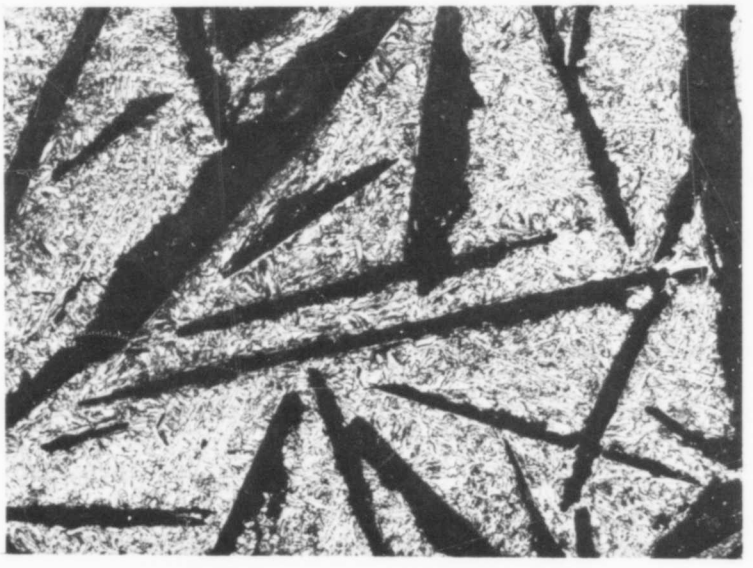

Figure 48. Carbon-Saturated Melt at 3600°C, Quenched (C_{total} = 55 At%). X100

Primary Crystallized Graphite (Black Plates) and α-WC_{1-x} + WC Eutectic.

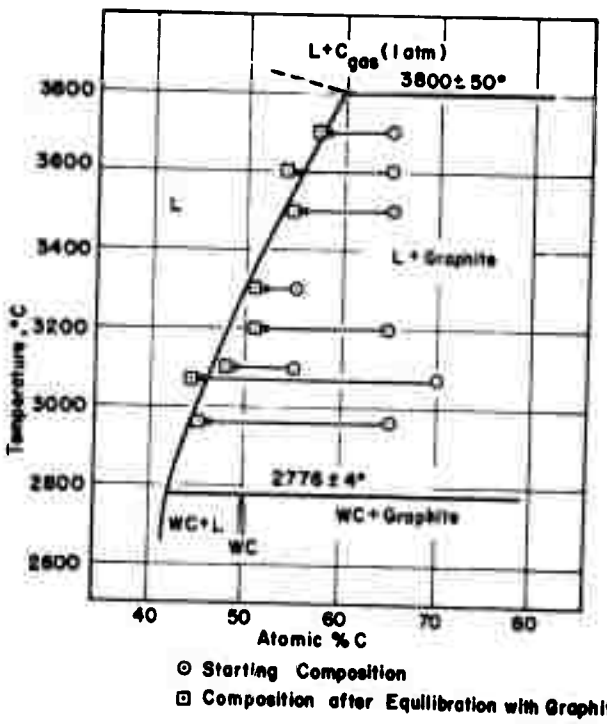

Figure 49. Tungsten-Carbon: Composition of the Graphite-Saturated Melt as a Function of Temperature.

Eight equilibration experiments were carried out, and the temperature range covered varied from 2950 to ~3750°C; the analytical results, summarized in the plot in Figure 49, show a nearly linear variation of the carbon-content of the graphite-saturated melt with the temperature. The liquidus line intersects the one atmosphere line of graphite at 3800°C and at a carbon concentration of approximately 60 atomic percent. No measurements could be carried out above

this temperature; the possible course of the isobaric (with respect to carbon) line estimated from partially assumed activities of carbon in the melt and available data for graphite, are indicated by the dotted line in Figure 49.

The experimental evidence is summarized in the proposed phase diagram for the tungsten-carbon system shown in Figure 1.

IV. SUPPLEMENTARY DATA ON THE MOLYBDENUM-CARBON SYSTEM

A. OBJECTIVE AND EXPERIMENTAL APPROACH

In a previously reported[3], complete treatment of the system, certain phase diagram details could not be delineated and proven to the desired degree of accuracy. Points which needed further affirmation included:

1. Proof for the assumption, that α-Mo_2C and β-Mo_2C, as well as the pair: η-MoC_{1-x} and α-MoC_{1-x} do exist as four distinct phases at high temperatures, and

2. Precise location of the eutectoid decomposition temperature of β-Mo_2C.

For α- and β-Mo_2C, a two-phased reaction process seems to be fairly well established from equilibration experiments under a temperature gradient[3]. However, independent confirmation by experiments carried out under isothermal conditions proved to be desirable. Although there is little doubt, that the high temperature phases η-MoC_{1-x} and α-MoC_{1-x} exist as distinct phases at 2000°C, no direct experimental proof that this behavior persists to temperatures above 2200°C could be obtained.

As for the eutectoid decomposition temperature of β-Mo_2C, only rather gradual temperature arrests (wide separation between the reaction onsets on the heating and the cooling cycle) were obtained for alloys located close to the stoichiometric composition, whereas considerable interference occurred with slightly hyperstoichiometric alloys as a result of the decomposition reaction of η-MoC_{1-x}.

Among the various approaches for positive phase distinction, the diffusion couple technique, used successfully by G. Santoro and H. B. Probst[45, 46] in the investigation of tantalum-carbon alloys, seemed to be the most attractive.

In the actual experimentations, diffusion couples Mo-C, α-Mo_2C-C, and η-MoC_{1-x} were investigated. The base alloys were prepared by hot-pressing powders (< 44 μ) of the corresponding compositions in graphite dies. After hot-pressing, the excess graphite was cut off from both ends of the specimens, and the alloy plugs were then equilibrated under high purity helium. For excess molybdenum-containing diffusion couples, 2200 and 2300°C were chosen as equilibration temperatures, while all others were run in the vicinity of 2300°C only.

The α-β- Mo_2C phase reaction was studied by differential-thermoanalytical means on chemically analyzed and carefully prehomogenized alloys. The main effort in the studies concentrated on alloys having compositions between 31 and 34 At% C. The solid state reactions in higher carbon alloys (34 to 40 At% C) were studied as a function of the heating and cooling rate, since the sluggish decomposition of η-MoC_{1-x} at temperatures below 1650°C caused some interference with the α-β-Mo_2C reaction.

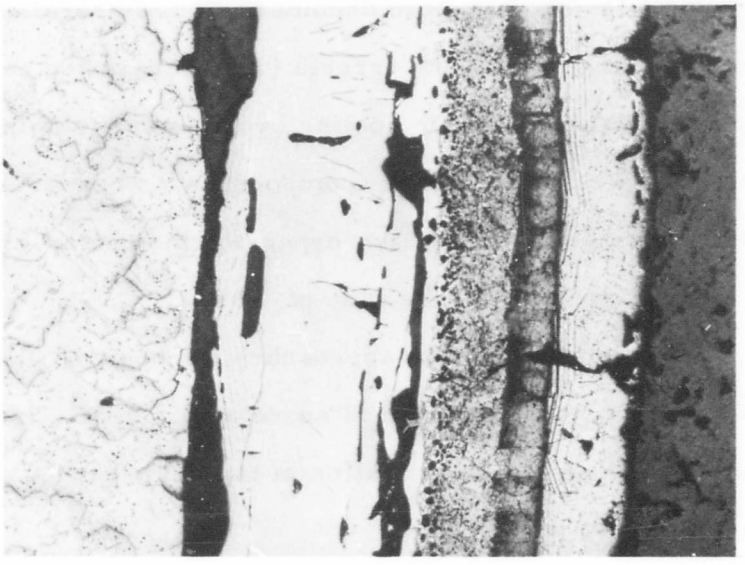

A G R B G C D E F

Figure 50. Molybdenum-Carbon Diffusion Couple (22 Minutes at 2200°C, Cooled at 14°C per Second). X100

A...Molybdenum

B... α-Mo_2C

C... β-Mo_2C

D... η-MoC_{1-x}

E... α-MoC_{1-x}

F...Graphite

R...Zone with Molybdenum Precipitations from Substoichiometric Mo_2C.

G...Gaps Due to Differential Thermal Expansion.

B. RESULTS

1. Diffusion Couple Experiments

A typical result of a diffusion couple experiment performed at 2200°C is shown in Figure 50. A similar arrangement of the phases was observed in the analogous diffusion experiment performed at 2300 °C (Figure 51), the only difference being that the major part of the center portion consists of the Mo + Mo_2C Eutectic (Figure 52).

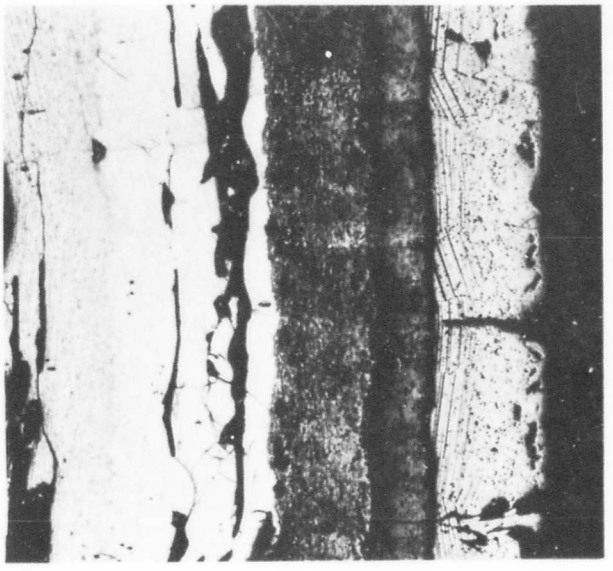

Figure 51. Molybdenum-Carbon Diffusion Couple, (14 Minutes at 2300°C). X100

Legend: See Figure 50.

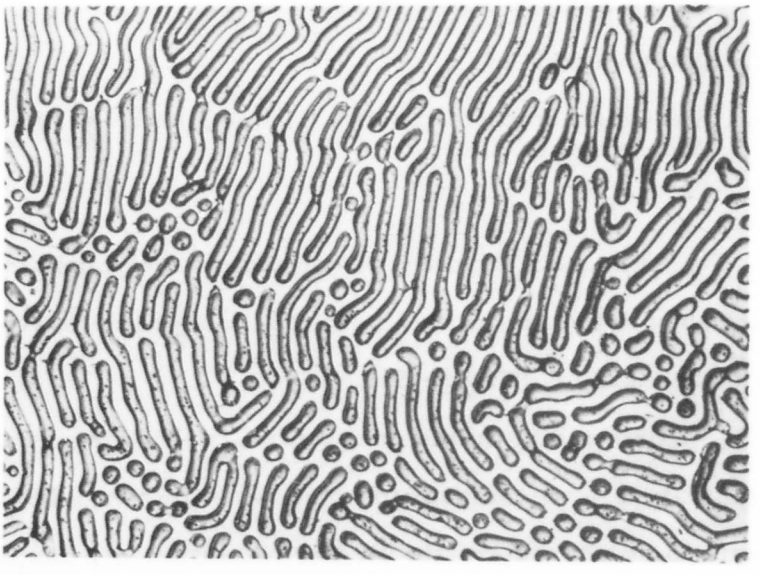

Figure 52. Section of Molten Center Portion of the Sample Shown in Figure 51. X375

Mo + Mo_2C Eutectic.

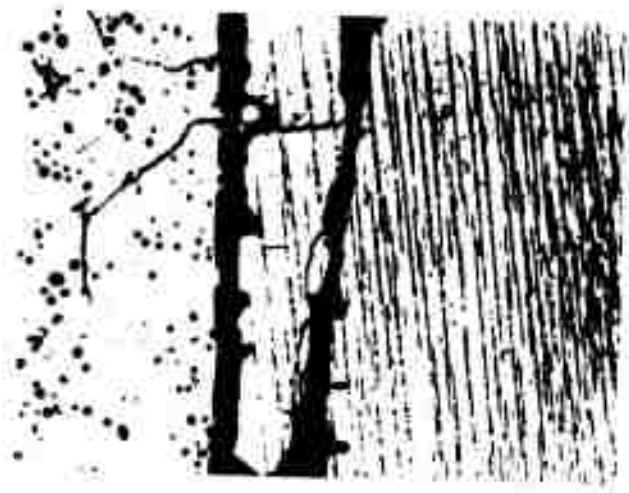

A B

Figure 53. Molybdenum-Carbon Diffusion Couple. Enlarged View of the Mo-Mo_2C Interface of the Sample Shown in Figure 50. X400

A...Molybdenum

B...Substoichiometric (26 At% C) Mo_2C with Mo-Precipitations.

The areas adjacent to the excess molybdenum containing center part show the typical unidirectional Mo-precipitations from substoichiometrical Mo_2C (Figure 53).

Proceeding to the next interface (Figures 54 and 55) we notice a veinlet-type of decomposition structure for the β-Mo_2C phase, which seems to be characteristic for the transition α-β-Mo_2C. The α-Mo_2C quasi precipitates temperature-dependently out of the β-Mo_2C phase until the conversion is complete, i.e. the β-phase has completely vanished. α- and

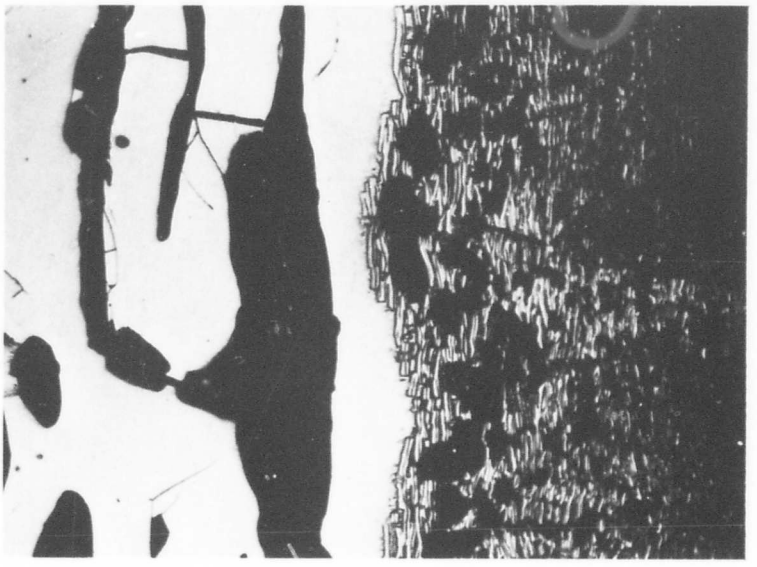

Figure 54. Molybdenum-Carbon Diffusion Couple, X400
Interface B-C of the Sample in Figure 51.

α-Mo_2C (Light), and β-Mo_2C (Decomposed).
Black: Gaps Close to the α-β-Mo_2C Interface.

β-Mo_2C must exhibit quite different thermal expansion characteristics, since both phases are usually separated by large gaps which had formed during cooling (Figure 55).

The type of decomposition structure for β-Mo_2C shown in the previous figures gradually disappears and is replaced by a nearly homogeneous structure towards somewhat higher carbon contents (Figure 56). The varying appearance of the decomposition structure of β-Mo_2C almost suggests the existence of two separate phases, although a closer inspection of the diffusion layers reveals, that only a single phase is involved. This is probably more clearly depicted in the micrograph of Figure 57, showing a single β-Mo_2C grain traversing the whole diffusion layer.

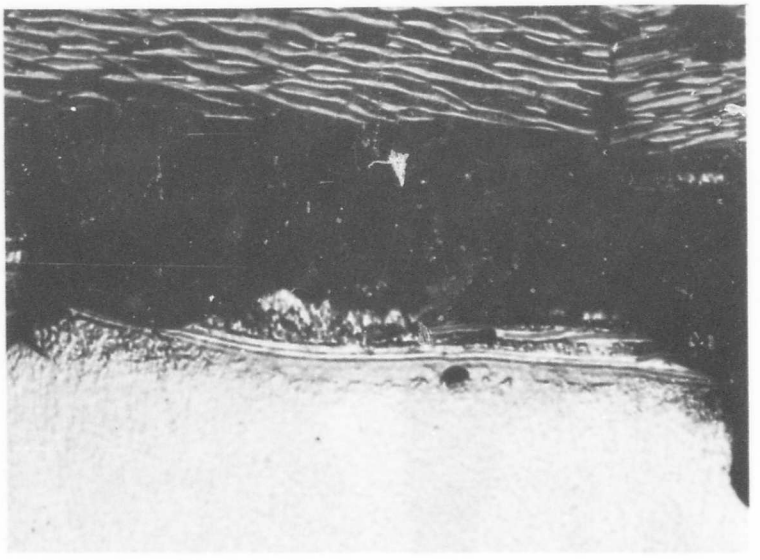

Figure 55. Molybdenum-Carbon Diffusion Couple X400
Sample of Figure 52, Interface B-C.

α- and β-Mo_2C with Separating Gap Due to Different Thermal Expansion of Both Phases.

A...α-Mo_2C

B...Gap

C...β-Mo_2C (Transformed)

From the two remaining phases, η-MoC_{1-x} can be easily identified by its characteristic decomposition pattern[3] as forming the diffusion zone next to β-Mo_2C.

As for the cubic (B1) high temperature phase, the conditions are not yet as clear, since in the molybdenum-carbon diffusion couples, only a very thin outer layer (adjacent to graphite) with a somewhat different decomposition structure, and separated by a regular crack zone from the η-phase, was observed (Figure 58).

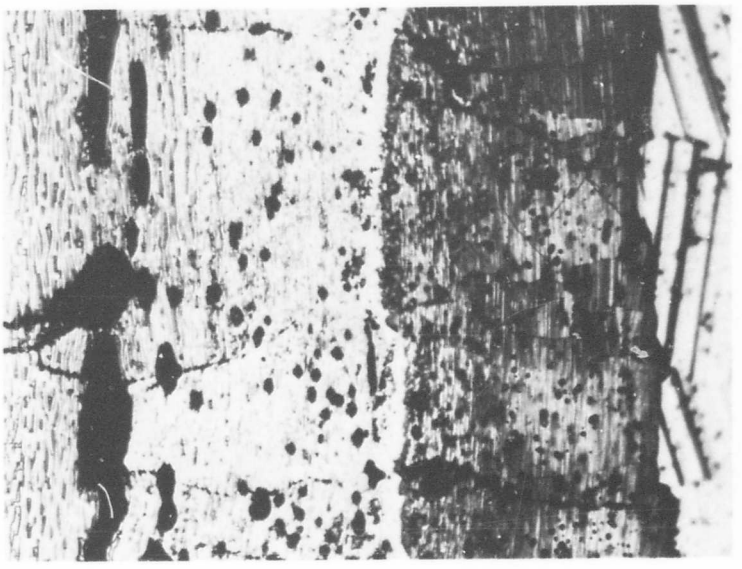

A B C D

Figure 56. Molybdenum-Carbon Diffusion Couple X400
Enlarged View of Zone B, and Interface C-D.

A. Compositions Within the Two-Phase Range α-β- Mo_2C("Quasiprecipitation" of α-Mo_2C).

B. Compositions Close to the Eutectoid, β-Mo_2C Only Partially Decomposed.

C. Hypereutectoid Compositions. Eutectoid Decomposition Preceded by Unidirectional Precipitation of η-MoC_{1-x}.

D. η-MoC_{1-x}.

The fact, that only a relatively thin layer of cubic phase had formed, suggests a much slower carbon transport through α-MoC_{1-x} as compared to the lower-carbon phases. In order to reduce the overall carbon drain into the interior and therefore to increase the relative layer thickness of the cubic phase, diffusion couples consisting of higher-carbon phases and graphite were prepared. The results

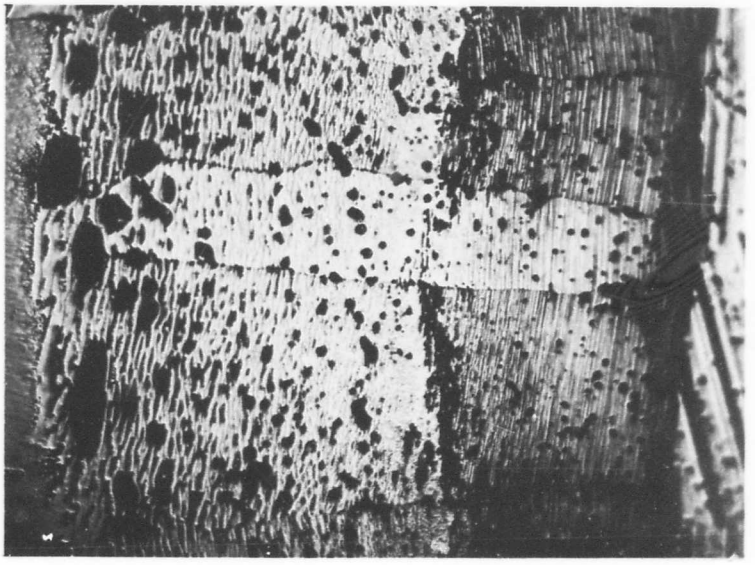

Figure 57. Molybdenum-Carbon Diffusion Couple, Sample of Figure 52. X400

Enlarged View of Interface B-C, Zone C, and Interface C-D.

Note β-Mo_2C Grain Traversing the Whole β-Mo_2C Diffusion Layer.

(Figures 59 through 63) are in favor of η-MoC_{1-x} and α-MoC_{1-x} existing as distinct phases at high temperatures, and also confirm the previous findings on the lower-carbon phases. The metallographic results were independently counterchecked by X-ray analysis performed on the individual layers of the dissected samples.

2. Extended DTA-Studies of the α-β-Mo_2C Phase Reaction

As discussed earlier, previous experiments[3] involved a certain ambiguity in the selection of the temperature for the eutectoid decomposition of β-Mo_2C, since representative and defined DTA-thermograms were available for the stoichiometric compositions only.

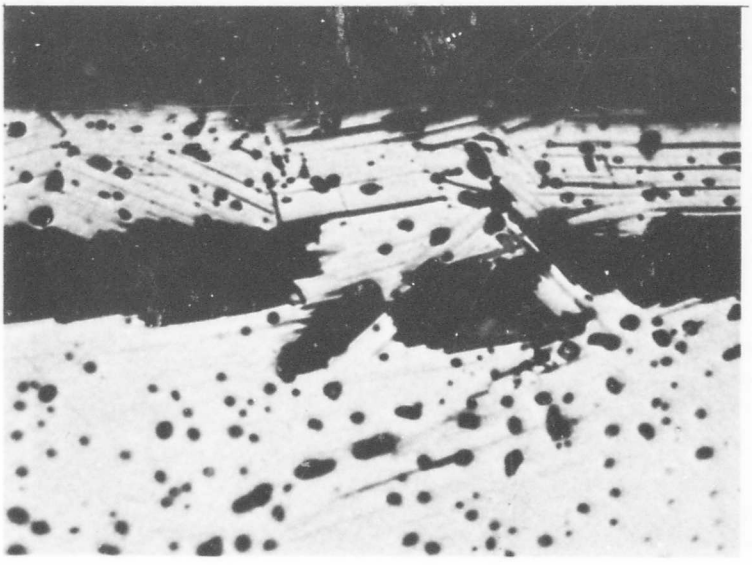

Figure 58. Sample of Figure 52, Interface D-E. X100

D...η-MoC_{1-x}

E... α-MoC_{1-x}

G...Gap Formed Due to Different Thermal Expansion.

The present re-evaluation of the phase relations in the critical concentration area covered the composition range from 29 to 39 atomic percent carbon. The concentration spacing of the analyzed test specimens was approximated one atomic percent.

Within the sensitivity limits of the DTA-setup ($\approx$ 0.1 cal enthalpy change per gram sample material) no signs of an isothermal solid state phase change could be observed in substoichiometric (< 32 At% C) Mo_2C; the shape of the curves do indicate, however, an anomalous enthalpy change over a wide temperature span (Figures 64 and 65),

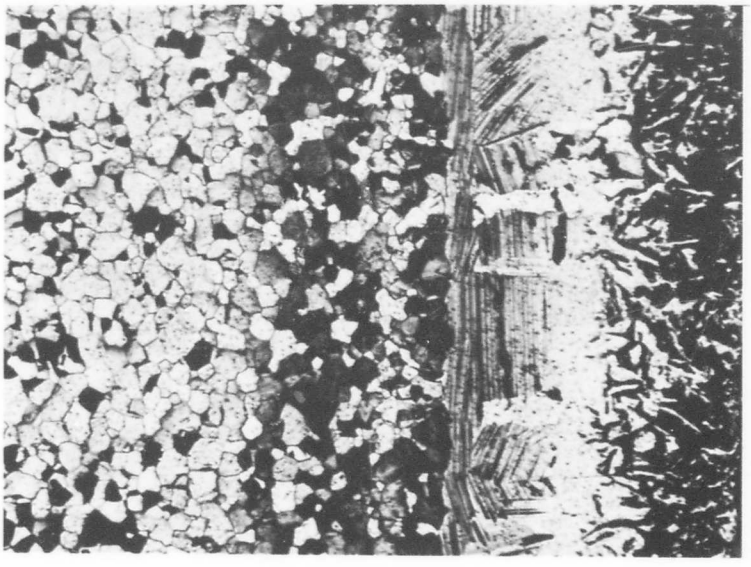

A B B' B" C D

Figure 59. Diffusion Couple (Mo-32 At% C)-Graphite 15 Minutes at 2300°C, Cooled with 14°C per Second. X50

A...α-Mo_2C

B...β-Mo_2C, Decomposed Compositions from Within the Two-Phase Field α-β-Mo_2C.

B'..β-Mo_2C, Partially Decomposed. Composition Close to the Eutectoid.

B"..β-Mo_2C, Partially Decomposed. Hypereutectoid Compositions, with η-MoC_{1-x} Precipitations.

C...η-MoC_{1-x}, to a Large Degree Decomposed (X-ray).

D...α-MoC_{1-x}, Decomposed into η-MoC_{1-x}, Mo_2C, and C. Heavily Attacked by Etchant.

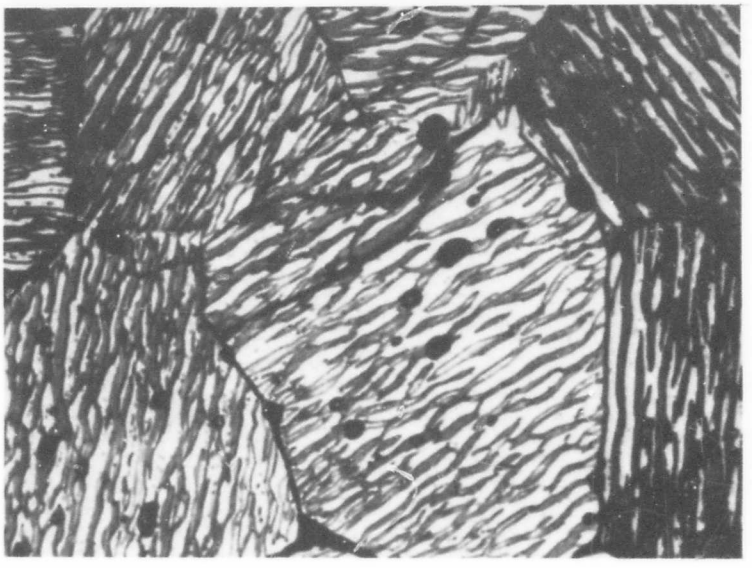

Figure 60. Sample from Figure 59. X1000

Zone B: β-Mo_2C, Transformed into α-Mo_2C.

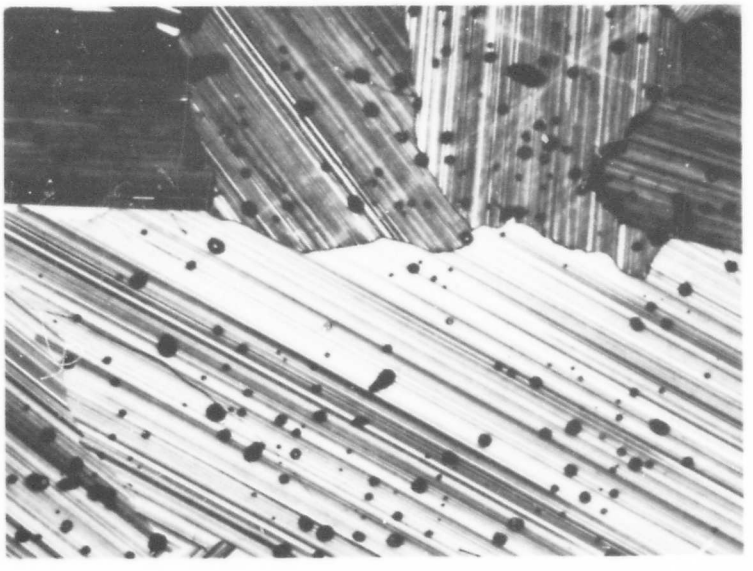

Figure 61. Sample From Figure 59. Interface B"—C X600

B"... β-Mo_2C with Unidirectional η-MoC_{1-x} Precipita-

C ...η-MoC_{1-x}, Partially Decomposed.

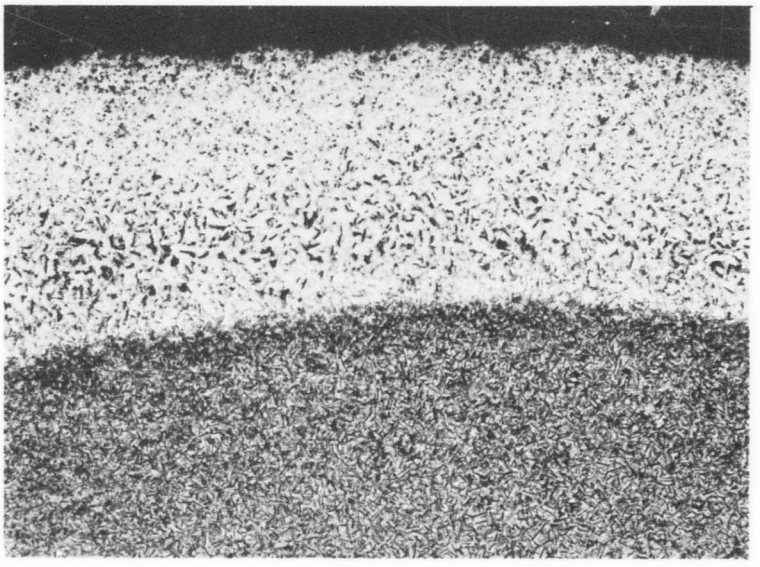

Figure 62. Diffusion Couple η-MoC_{1-x} (39 At% C)-Graphite X25
15 Minutes at ~2330°C, Cooled at 15°C per Second.

A...η-MoC_{1-x}, Decomposed.

B...α-MoC_{1-x}, Decomposed.

a b

Figure 63. Sample from Figure 62. X400

a. Average Appearance of Zone A (Decomposed η-MoC_{1-x})

b. Average Appearance of Zone B (Decomposed α-MoC_{1-x})

indicating that the previously discussed[3] possibility of a homogeneous order-disorder (changes of short-range order) reaction might exist.

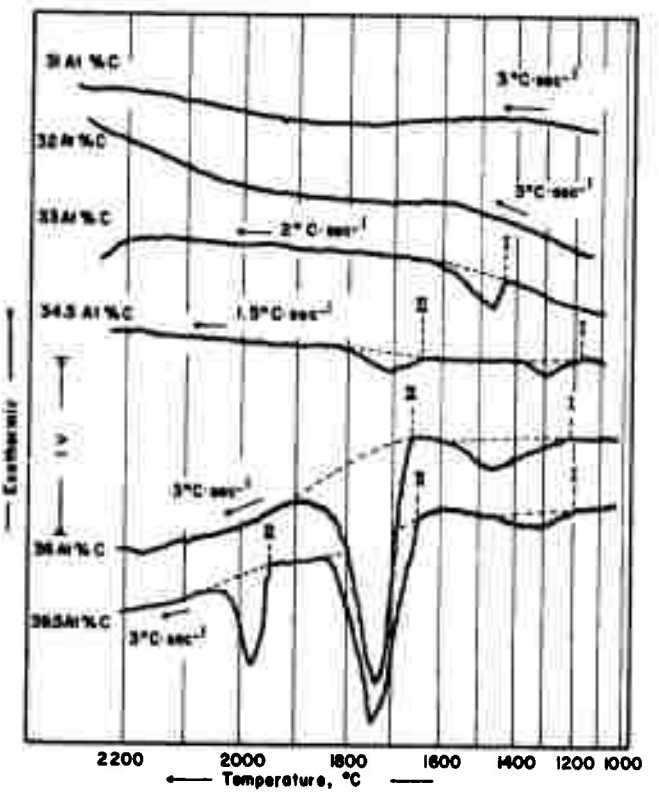

Figure 64. DTA-Thermograms (Heating) of Molybdenum-Carbon Alloys.

I. α-β-Mo_2C Phase Reaction

II. β-$Mo_2C + C \rightarrow \eta$-$MoC_{1-x}$

III. η-$MoC_{1-x} + C \rightarrow \alpha$-$MoC_{1-x}$

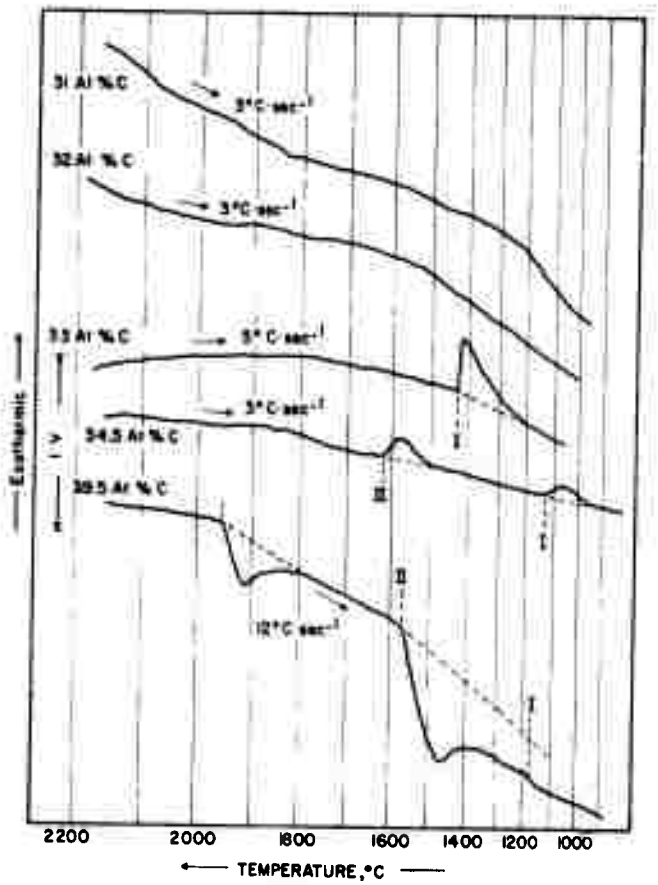

Figure 65. DTA-Thermograms (Cooling) of Molybdenum-Carbon Alloys.

I. α-β-Mo_2C Phase Reaction

II. η-$MoC_{1-x} \rightarrow \beta$-$Mo_2C + C$

III. α-$MoC_{1-x} \rightarrow \eta$-$MoC_{1-x} + \beta$-$Mo_2C$

In the alloy with 33 atomic percent carbon, a sharp and rapid transition occurs in the temperature range from 1420 to 1450°C (Figure 64 through 67). Increase of the carbon content to 34.5 atomic percent causes this reaction to shift down to approximately 1200°C (Figure 64, 65 and 68).

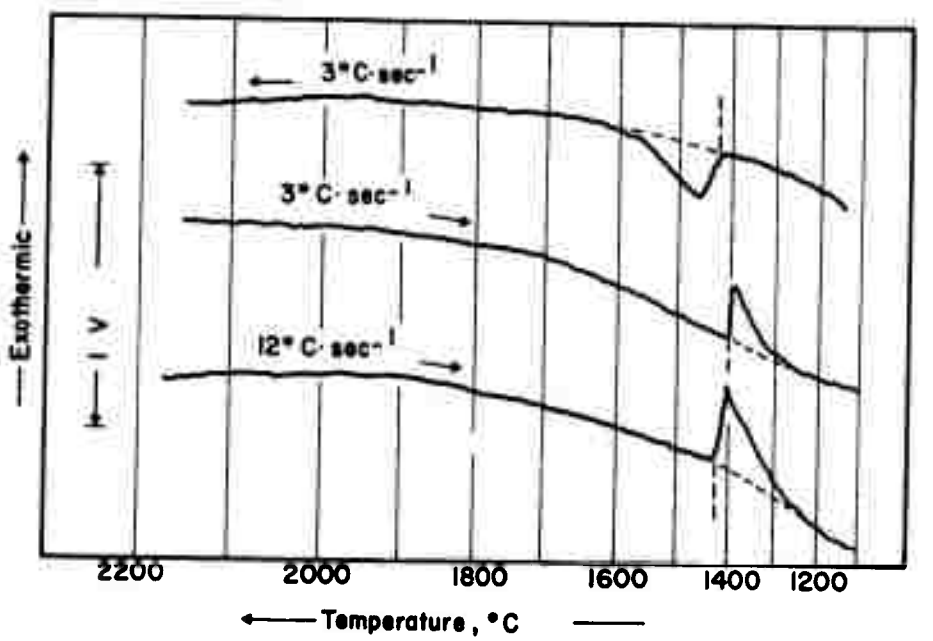

Figure 66. α-β-Mo_2C Phase Reaction in a Mo-C Alloy with 33 Atomic Percent Carbon.

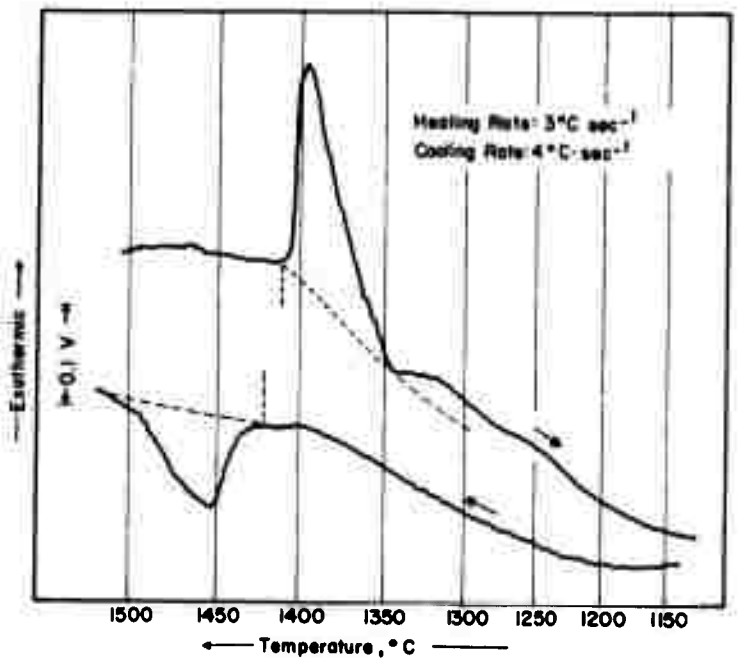

Figure 67. Sample of Figure 66, High Sensitivity Scale.

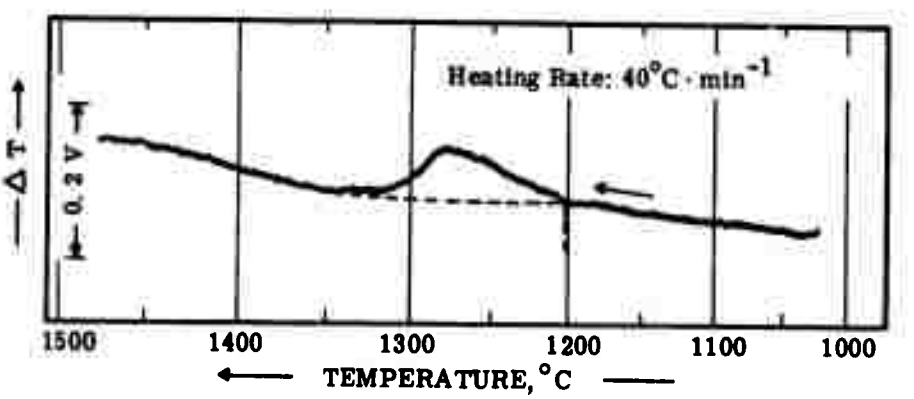

Figure 68. α-β-Mo_2C Phase Reaction in a Mo-C Alloy with 34.5 Atomic Percent Carbon.

(High Sensitivity Setting, Expanded Temperature Scale)

The decomposition of β-Mo_2C at hypereutectic compositions proceeds fairly sluggishly, as evidenced by the delay of the reaction on the down-cycle at slightly increased cooling speeds. We recall, that the same behavior was noticed in the

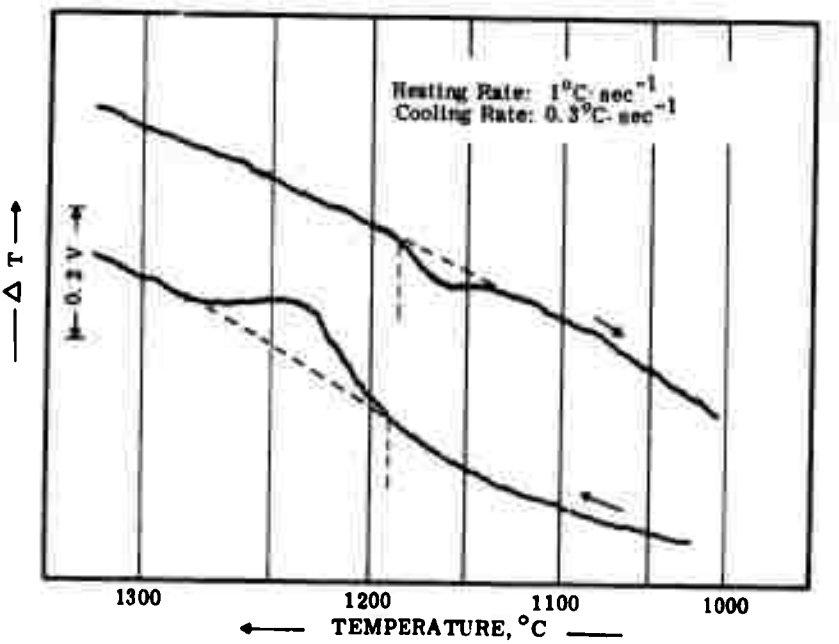

Figure 69. α-β-Mo_2C Phase Reaction in a Mo-C Alloy with 38.5 Atomic Percent Carbon.

metallographic examination of the diffusion couples (Figures 56 and 57). The second thermal arrest at ~1650°C (Figure 64 and 65) observed in the specimen with 34.5 atomic percent carbon stems from the formation (heating) or decomposition (cooling) of the η-MoC_{1-x}-phase, i.e. this composition already is hypereutectoidic.

The temperatures observed for the η-MoC_{1-x} and β-Mo_2C eutectoidic phase reactions show fairly good constancy in the still higher-carbon alloys (Figures 64, 65, and 69). We also note from the DTA-thermogram of the alloy with 39.5 atomic percent carbon, that in addition to the η-MoC_{1-x} solid state reaction, the α-MoC_{1-x} peak appears at temperatures slightly above 1900°C.

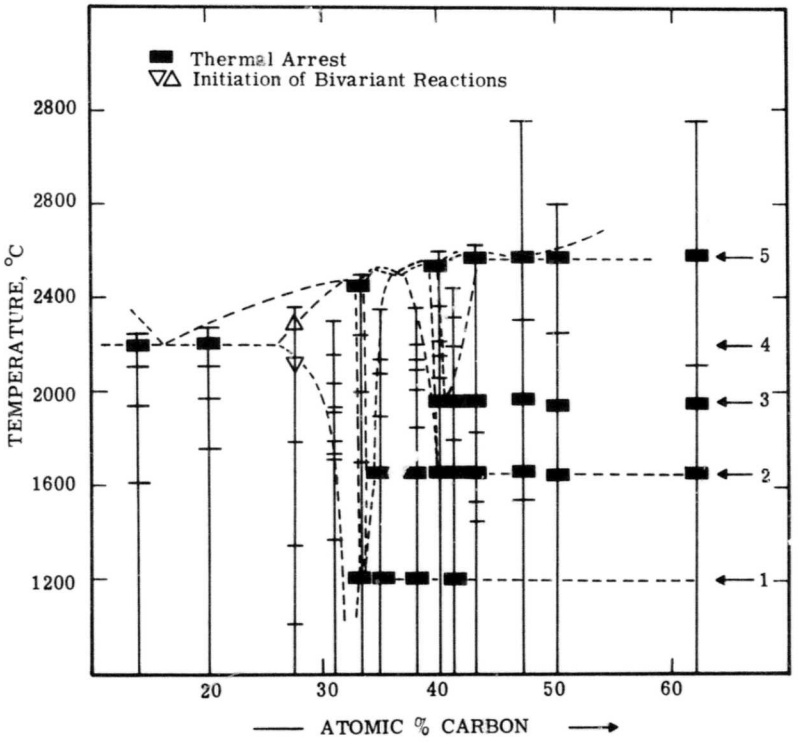

Figure 70. Molybdenum-Carbon: Summary of Differential-Thermoanalytical Investigations.

Isothermal Reactions

(1) α-$Mo_2C + C \rightleftarrows \beta$-$Mo_2C$

(2) β-$Mo_2C + C \rightleftarrows \eta$-$MoC_{1-x}$

(3) η-$MoC_{1-x} + C \rightleftarrows \alpha$-$MoC_{1-x}$

(4) Mo + α-Mo C $\rightleftarrows$ L (Eutectic Reaction)

(5) α-MoC_{1-x} + C(gr.) $\rightleftarrows$ L (Eutectic Reaction)

The differential-thermoanalytical investigations, including the present as well as previous[3] results, are summarized in the diagram shown in Figure 70.

The results obtained in the present investigation are in general confirmation to the phase diagram data presented in the earlier system report and may serve as valuable supplemental information on the rather peculiar and complex phase relations in this system.

V. DISCUSSION

The maximum solidus temperatures for W_2C and WC, as well as the temperatures for the W-W_2C reaction isotherm obtained in this investigation are in fair agreement with previously reported, partial phase diagram data (Table 3). The eutectoid point of the cubic high temperature phase is in confirmation to the results by R. T. Doloff and R.V. Sara[4, 5]. Some differences with the results obtained by the latter authors are found in the high temperature-carbon rich portion of the system, as evidenced by a comparison of the two diagrams (Figures 1 and 3). A possible explanation of the discrepancies may be sought in the aforementioned segregation of the peritectic melt from the lower-density graphite, thus simulating two separate reactions on the cooling cycles in the DTA-experiments.

One interesting result emerging from the present reinvestigation concerns the confirmation of the polymorphic phase change in W_2C, which had not been contested since the original observations by F. Skaupy[6] and K. Becker[7, 8, 9]. Although from the investigations in the binary as well as ternary systems, it seems to be fairly well established, that the

phase changes in the Me_2C phase are associated with disordering reactions occurring in the carbon sublattice and do not involve a structural change of the metal host lattice, independent confirmation of these conclusions by high temperature neutron diffraction techniques would be highly desirable.

REFERENCES

1. E. Rudy: 2nd Progress Report AF 33(615)-1249 (Sept 1964).

2. E. Rudy and D.P. Harmon, 3rd Progress Report, AF 33(615)-1249 (April 1965).

3. E. Rudy, St. Windisch and Y.A. Chang: AFML-TR-65-2, Part I, Vol. I. (Jan 1965).

4. R.T. Doloff and R.V. Sara: WADD TR 60-143 (1961), Part II.

5. R.V. Sara: J. Am. Ceram. Society, 48 (1965), 251.

6. F. Skaupy: Z. Elektrochem. 33 (1927), 487.

7. K. Becker: Z. Elektrochem., 34 (1938), 640.

8. K. Becker: Z. Physik, 51 (1928), 481.

9. K. Becker: Z. Metallkde., 20 (1928), 437.

10. E. Rudy and D.P. Harmon: AFML-TR-65-2, Part I, Vol.V.(Sept. 1965).

11. H.D. Heetderks, E. Rudy, and T. Eckert: AFML-TR-65-2, Part III, Vol. I. (May 1965).(Planseeber.Pulvermet., in print).

12. W.P. Sykes: Trans. Am. Soc. Steel Treat. 18 (1930), 968.

13. A. Westgren and G. Phragmén: Z. anorg.allg.Chemie, 156 (1926), 27.

14. J. Leciewicz: Polish Acad.Sci.Inst.Nucl.Res. Report No.142/I-B.

15. E.K. Storms: Critical Review of Refractories, LA - 2942 (Aug 1964).

16. L.N. Butorina and Z.G. Pinsker: Soviet Physics, Crystallography, 5, (1960), 560.

17. For an exhaustive compilation and discussion of earlier work. compare: R. Kieffer and F. Benesovsky, Hartstoffe (Wien, Springer, 1963).

18. P. Rantala and J.T. Norton: Plansee Proceedings of the I. Plansee Seminar, Reutte, Tirol, 1959, 303.

19. H. Nowotny, E. Parthé, R. Kieffer, and F. Benesovsky: Z. Metallkde, 45 (1954), 97.

Reference (cont.)

20. G.W. Orton: Thesis, Ohio State University, 1961.

21. K. Kirner: 1957 (Work quoted in R. Kieffer and F. Benesovsky, Hartstoffe, Wien Springer, 1963).

22. G. Lautz and D. Schneider: Z. Naturforschung 16a (1961), 1368.

23. H.J. Goldschmidt and J.A. Brand: J. Less Common Metals, 5 (1962), 181.

24. H. Pfau and W. Rix: Z. Metallkde, 45 (1954), 116.

25. Compare also M. Hansen: Constitution of Binary Alloys, (McGraw-Hill, 1958).

26. G. Hägg: Z. Physik. Chem. Biz (1931), 33.

27. W. B. Pearson: Handbook of Lattice Spacings and Structures of Metal and Alloys (Pergamon, New York, 1958).

28. O. Ruff and R. Wunsch: Z. anorg.allg.Chem. 85 (1914), 292.

29. K. Becker and R. Hölbling: Z. angew. Chem. 40 (1927), 511.

30. J.L. Gregg and C. W. Küttner: Trans.Am.Inst.Min.Met.Eng. 88 (1929), 581.

31. S.L. Hoyt: Trans.Am.Inst.Min.Met.Engrs. 89 (1930), 9.

32. M.R. Andrews and S. Dushman: J. Franklin Inst. 192 (1921), 545.

33. C. Agte and H. Alterthum: Z.Tech.Phys. 11 (1930), 185.

34. B.T. Barnes: J. Phys. Chem. 33 (1929), 688.

35. E. Friedrich and L. Sittig: Z.anorg. Chem. 144 (1923), 184.

36. M.R. Nadler and C.P. Kempter: J. Phys.Chem. 64, (1960) 1468

37. H. Drainer and K. Konopicky: Berg. und hüttenmänn. Mh. 92 (1947), 166.

38. E. Rudy, F. Benesovsky, and L. Toth: Z.Metallkde. 54 (1963), 345.

39. J.J. Lander and L.H. Germer: Trans. AIME 175 (1948), 648.

40. H. Krainer: Arch. Eisenhüttenwesen 21 (1950), 119.

References (cont.)

41. A. G. Metcalfe: Met. Treat. 13 (1946), 127.

42. E. Rudy and G. Progulski: (in preparation for print).

43. E. Rudy and D.P. Harmon: AFML-TR-65-2, Part I, Vol. V. (Sept. 1965).

44. E. Rudy and Y.A. Chang: Plansee Proc. of the V. Plansee Seminar (1964).

45. G. Santoro and H. B. Probst in: W. Mueller (Editor): "Advances in X-Ray Analysis", Vol. 7 (1963), 126, (Plenum Press, New York).

DOCUMENT CONTROL DATA - R&D

(Security classification of title, body of abstract and indexing annotation must be entered when the overall report is classified)

1. ORIGINATING ACTIVITY *(Corporate author)*
Aerojet-General Corporation
Materials Research Laboratory
Sacramento, California

2a. REPORT SECURITY CLASSIFICATION
Unclassified

2b. GROUP
N.A.

3. REPORT TITLE
Ternary Phase Equilibria in Transition Metal-Boron-Carbon-Silicon Systems
Part I. Related Binary Systems: Vol. VI. W-C System; Supplemental Information on the Mo-C System

4. DESCRIPTIVE NOTES *(Type of report and inclusive dates)*

5. AUTHOR(S) *(Last name, first name, initial)*
E. Rudy
St. Windisch
J. R. Hoffman

6. REPORT DATE	7a. TOTAL NO. OF PAGES	7b. NO. OF REFS
January 1966	79	45

8a. CONTRACT OR GRANT NO.	9a. ORIGINATOR'S REPORT NUMBER(S)
AF 33(615)-1249	AFML-TR-65-2 Part I, Vol. VI.
b. PROJECT NO. 7350	
c. Task No. 735001	9b. OTHER REPORT NO(S) *(Any other numbers that may be assigned this report)*
d.	N.A.

10. AVAILABILITY/LIMITATION NOTICES
This document is subject to special export controls, and each transmittal to foreign governments or foreign nationals may be made only with prior approval of Metals & Ceramics Div., AF Materials Laboratory, Wright-Patterson, AFB, Ohio.

11. SUPPLEMENTARY NOTES

12. SPONSORING MILITARY ACTIVITY
AFML (MAMC)
Wright-Patterson AFB, Ohio 45433

13. ABSTRACT

The alloy system tungsten-carbon was investigated by means of X-ray, DTA, and melting point techniques on chemically analyzed alloys, and a complete phase diagram was established.

Supplementary investigations performed on the molybdenum-carbon system are in confirmation of our previous findings regarding the α-β-MoC_{1-x} phase separation as well as the phase relations between β- and η-MoC_{1-x}.

The results are discussed and compared with previously reported system data.

DD FORM 1 JAN 64 1473

Unclassified
Security Classification

Unclassified
Security Classification

14. KEY WORDS	LINK A		LINK B		LINK C	
	ROLE	WT	ROLE	WT	ROLE	WT
Binary Carbide Phase Equilibria Tungsten-Carbon						

INSTRUCTIONS

1. **ORIGINATING ACTIVITY**: Enter the name and address of the contractor, subcontractor, grantee, Department of Defense activity or other organization *(corporate author)* issuing the report.

2a. **REPORT SECURITY CLASSIFICATION**: Enter the overall security classification of the report. Indicate whether "Restricted Data" is included. Marking is to be in accordance with appropriate security regulations.

2b. **GROUP**: Automatic downgrading is specified in DoD Directive 5200.10 and Armed Forces Industrial Manual. Enter the group number. Also, when applicable, show that optional markings have been used for Group 3 and Group 4 as authorized.

3. **REPORT TITLE**: Enter the complete report title in all capital letters. Titles in all cases should be unclassified. If a meaningful title cannot be selected without classification, show title classification in all capitals in parenthesis immediately following the title.

4. **DESCRIPTIVE NOTES**: If appropriate, enter the type of report, e.g., interim, progress, summary, annual, or final. Give the inclusive dates when a specific reporting period is covered.

5. **AUTHOR(S)**: Enter the name(s) of author(s) as shown on or in the report. Enter last name, first name, middle initial. If military, show rank and branch of service. The name of the principal author is an absolute minimum requirement.

6. **REPORT DATE**: Enter the date of the report as day, month, year; or month, year. If more than one date appears on the report, use date of publication.

7a. **TOTAL NUMBER OF PAGES**: The total page count should follow normal pagination procedures, i.e., enter the number of pages containing information.

7b. **NUMBER OF REFERENCES**: Enter the total number of references cited in the report.

8a. **CONTRACT OR GRANT NUMBER**: If appropriate, enter the applicable number of the contract or grant under which the report was written.

8b, 8c, & 8d. **PROJECT NUMBER**: Enter the appropriate military department identification, such as project number, subproject number, system numbers, task number, etc.

9a. **ORIGINATOR'S REPORT NUMBER(S)**: Enter the official report number by which the document will be identified and controlled by the originating activity. This number must be unique to this report.

9b. **OTHER REPORT NUMBER(S)**: If the report has been assigned any other report numbers *(either by the originator or by the sponsor)*, also enter this number(s).

10. **AVAILABILITY/LIMITATION NOTICES**: Enter any limitations on further dissemination of the report, other than those imposed by security classification, using standard statements such as:

(1) "Qualified requesters may obtain copies of this report from DDC."

(2) "Foreign announcement and dissemination of this report by DDC is not authorized."

(3) "U. S. Government agencies may obtain copies of this report directly from DDC. Other qualified DDC users shall request through _____."

(4) "U. S. military agencies may obtain copies of this report directly from DDC. Other qualified users shall request through _____."

(5) "All distribution of this report is controlled. Qualified DDC users shall request through _____."

If the report has been furnished to the Office of Technical Services, Department of Commerce, for sale to the public, indicate this fact and enter the price, if known.

11. **SUPPLEMENTARY NOTES**: Use for additional explanatory notes.

12. **SPONSORING MILITARY ACTIVITY**: Enter the name of the departmental project office or laboratory sponsoring *(paying for)* the research and development. Include address.

13. **ABSTRACT**: Enter an abstract giving a brief and factual summary of the document indicative of the report, even though it may also appear elsewhere in the body of the technical report. If additional space is required, a continuation sheet shall be attached.

It is highly desirable that the abstract of classified reports be unclassified. Each paragraph of the abstract shall end with an indication of the military security classification of the information in the paragraph, represented as *(TS), (S), (C), or (U)*.

There is no limitation on the length of the abstract. However, the suggested length is from 150 to 225 words.

14. **KEY WORDS**: Key words are technically meaningful terms or short phrases that characterize a report and may be used as index entries for cataloging the report. Key words must be selected so that no security classification is required. Identifiers, such as equipment model designation, trade name, military project code name, geographic location, may be used as key words but will be followed by an indication of technical context. The assignment of links, rules, and weights is optional.

Unclassified
Security Classification